Research Scholars **Investigators**

Hsiu-Yu Yu ***Portonovo Ayyaswamy***

Ramakrishnan Natesan ***David Eckmann***

Arijit Sarkar ***Vladimir Muzykantov***

Helena Vitoshkin ***Russ Composto***

Yaohong Wang ***Ravi Radhakrishnan****

* Associate Professor of Bioengineering

www.seas.upenn.edu/~biophys

rradhak@seas.upenn.edu

Insilico Pharmacology

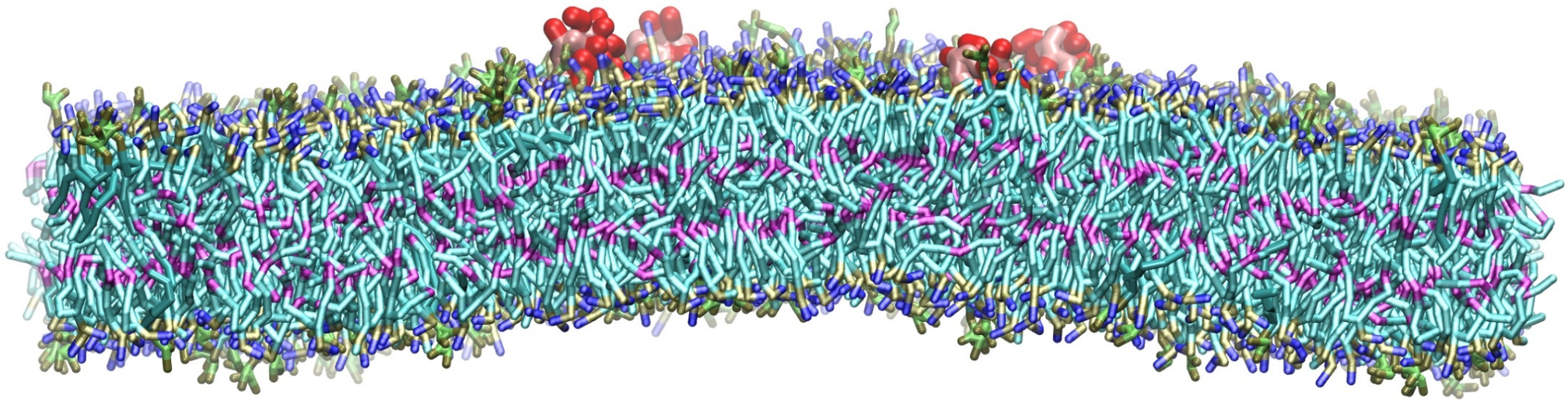

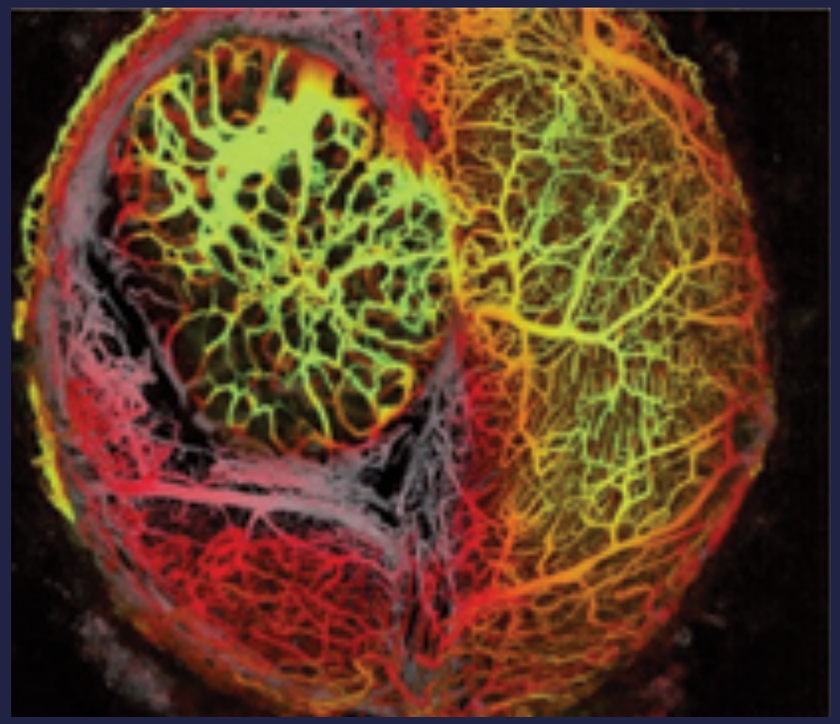

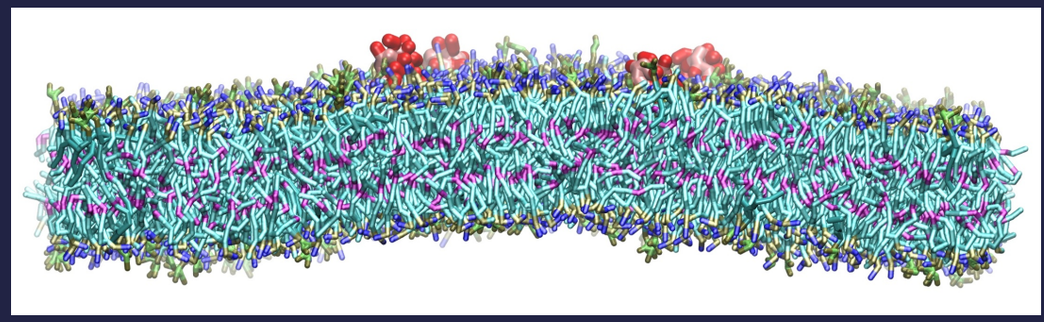

From Organ Scale to the Molecular Scale

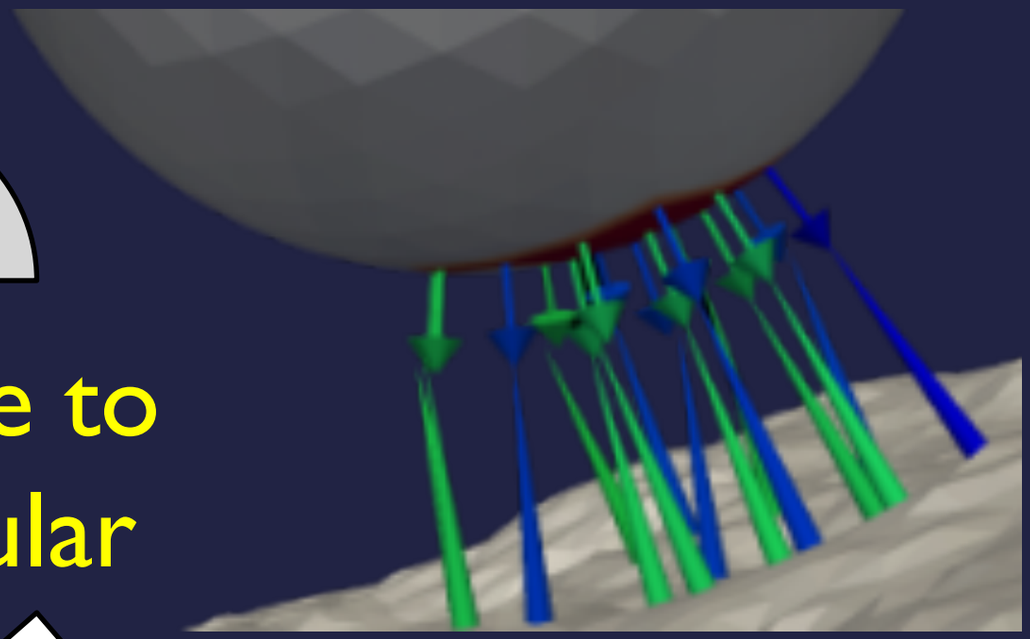

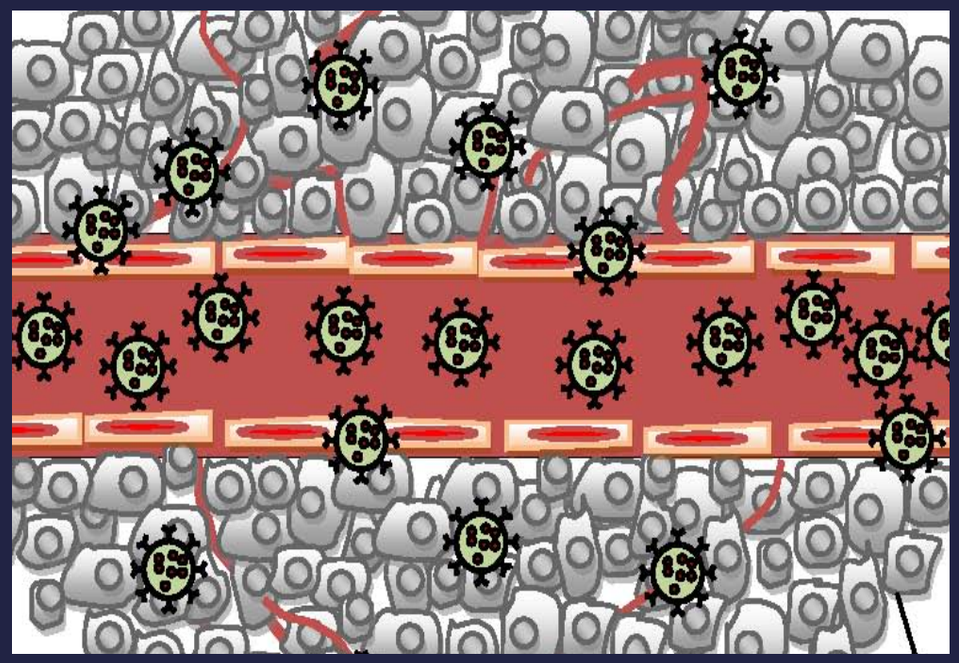

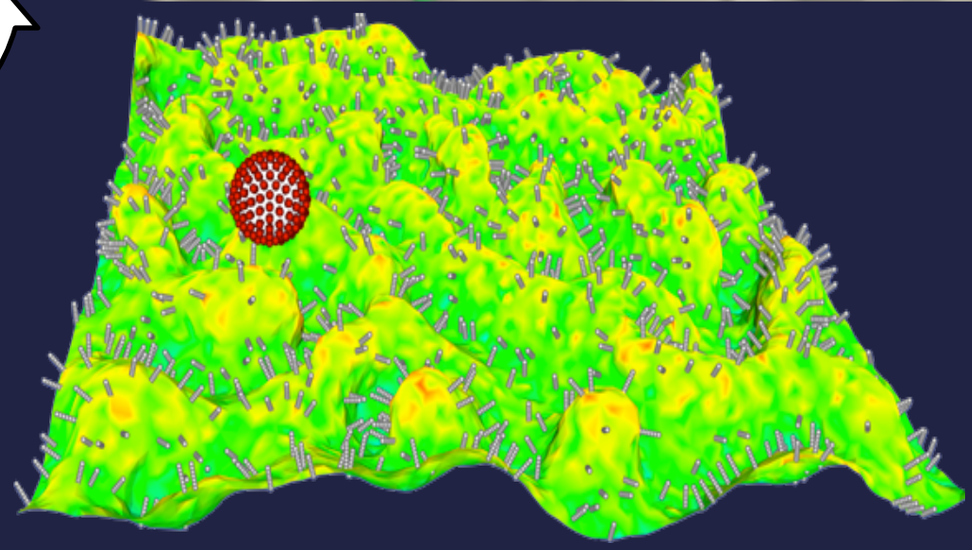

Objective: Next Generation Pharmacological Models For Targeted Drug Delivery

Outline

- Nanocarrier Binding Affinity
- Validation of Binding In Vivo
- Mean-Field Hydrodynamic Models of NC Motion
- Towards a System Wide Pharmacological Model
- Rigorous Treatment of Hydrodynamic Interactions

Minimal Model for Nanocarrier Adhesion

Objective: How do we quantify NC binding avidity to cells mediated by antibody-antigen interactions?

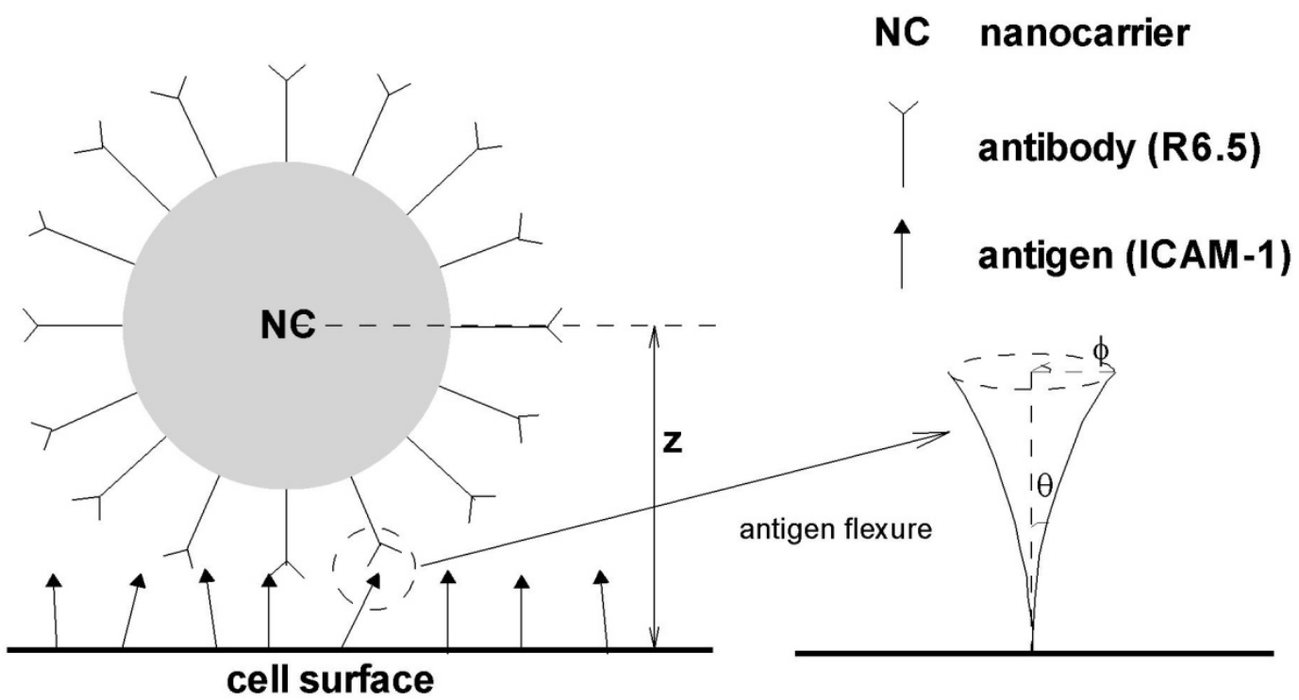

Antigen flexure

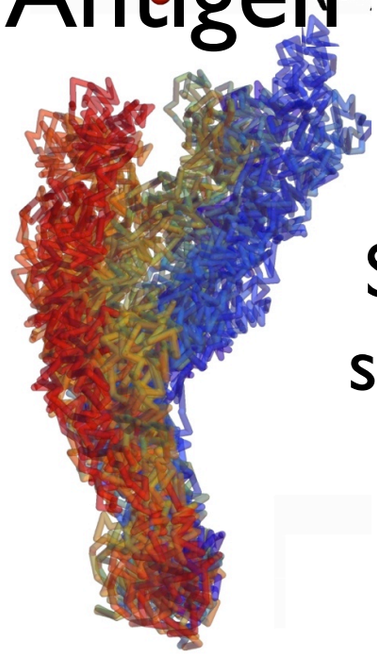

Superimposed snapshots from molecular dynamics

Liu *et al.* (2010) *PNAS* **107** 16530-16535

- Spherical 100nm NCs coated with uniformly distributed N_{ab} antibodies (Ab). The saturation Ab surface coverage (100%) σ_s=220Ab/NC in experiments.
- Antibody-antigen interaction is treated using the Bell model:

$$\Delta G_r(d) = \Delta G_0 + \frac{1}{2} k_0 d^2 \qquad k_0 : \text{bond force constant}$$

- Antigen flexure accounted for by orientational-bias MC sampling of θ and ϕ

Avidity: Absolute Free Energy of Binding of NC to Cells
Potential of Mean Force (PMF)

The binding avidity or association constant K_a directly measures the binding efficiency, for reaction

L+R ⇔ LR,

$$K_a = \frac{[\mathbf{LR}]}{[\mathbf{L}][\mathbf{R}]} = \frac{1}{[\mathbf{L}]} \times \frac{p_1}{p_0}$$

bound

unbound

Liu *et al.* (2010) *PNAS* **107** 16530-16535

The final form for K_a is:

Spatial Bond Distribution

PMF W(z)

$$K_a = \frac{(N_{ab}/N_b)\Delta\omega}{8\pi^2} \times \frac{A_{R,b}^{(1)} \times A_{R,b}^{(2)} \times \ldots \times A_{R,b}^{(N_b)}}{A_{R,ub}^{(1)} \times A_{R,ub}^{(2)} \times \ldots \times A_{R,ub}^{(N_b)}} \times A_{NC,b} \int e^{-\beta W(z)} dz$$

NC rotational entropy change

antigen entropy change

NC translational entropy change

Super-resolution florescence

Atomic Force Microscopy

Avidity is an Exactly Computable Quantity

Potential of Mean Force (σ_s=75%, 162Abs)

PMF profile

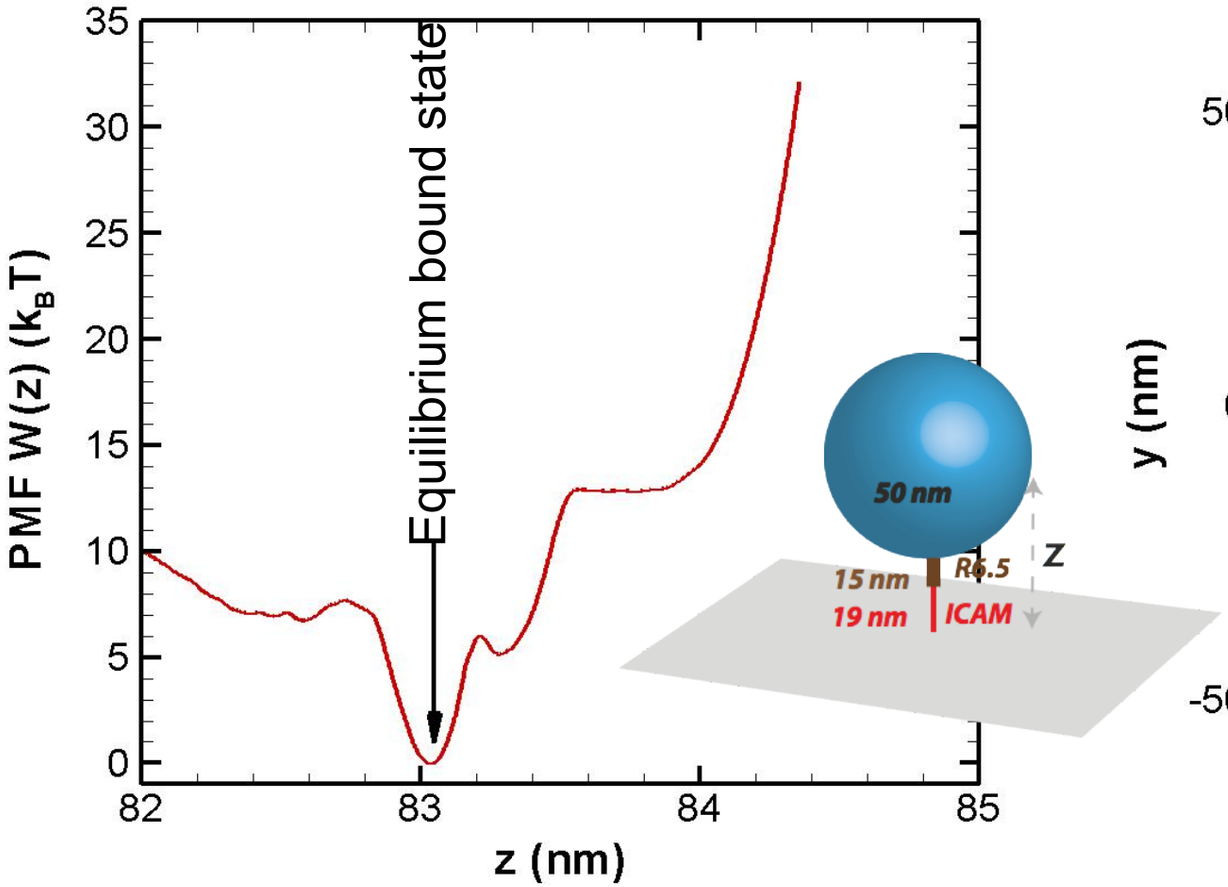

Spatial bond distribution

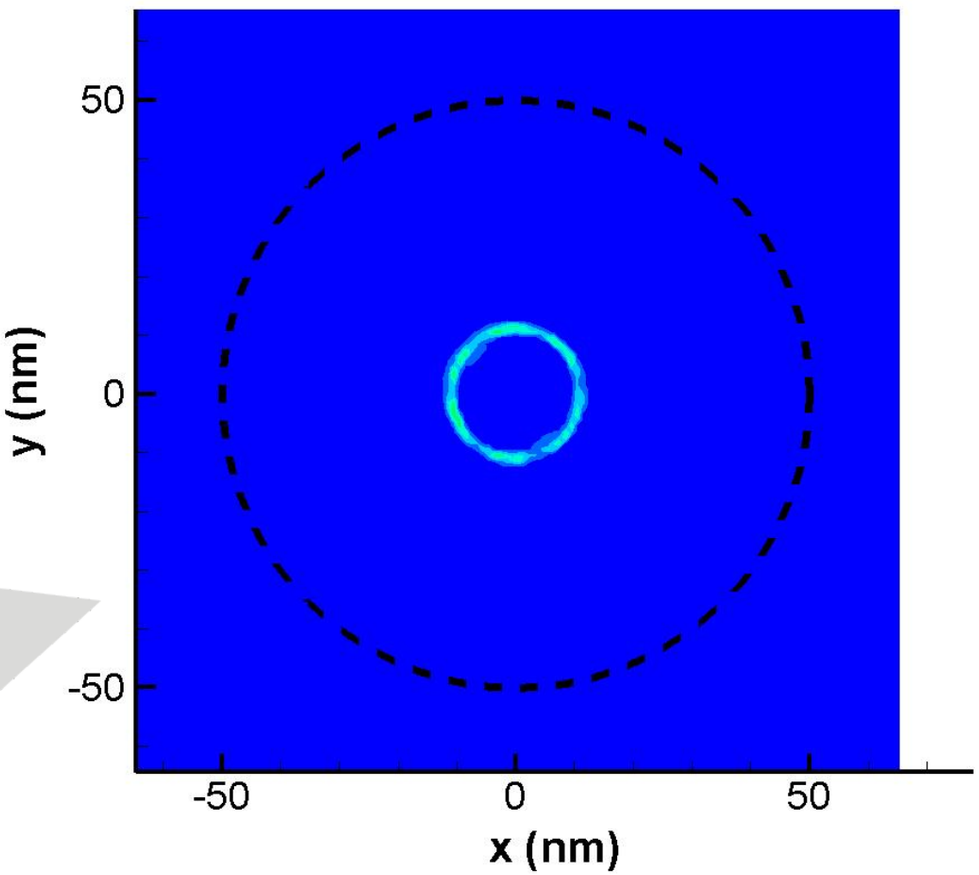

- 3 firm bonds formed with an energy well ~32k_BT

$$K_a = \frac{(N_{ab}/3)\Delta\omega}{8\pi^2} \times \frac{\pi(r_o^2 - r_i^2)(r_o - r_i)^4 \int e^{-\beta W(z)} dz}{(\pi r_o^2)^2}$$

$$= 5.9 \times 10^{10}\,\mathrm{nm}^3$$

Liu *et al.* (2010) *PNAS* **107** 16530-16535

- Annulus distribution with outer radius r_o=12.5nm and inner radius r_i=9.7nm
- The areas can be calculated as:

$$A_{R,b}^{(1)} = \pi r_o^2 \qquad A_{R,b}^{(2)} = \pi\left(r_o^2 - r_i^2\right)$$

$$A_{R,b}^{(3)} = A_{NC,b} = \left(r_o - r_i\right)^2$$

$$A_{R,ub}^{(1)} = A_{R,ub}^{(2)} = A_{R,ub}^{(3)} = \pi r_o^2$$

Energy Landscape for Adhesion

NC Dissociation Constant, K_d

Model prediction

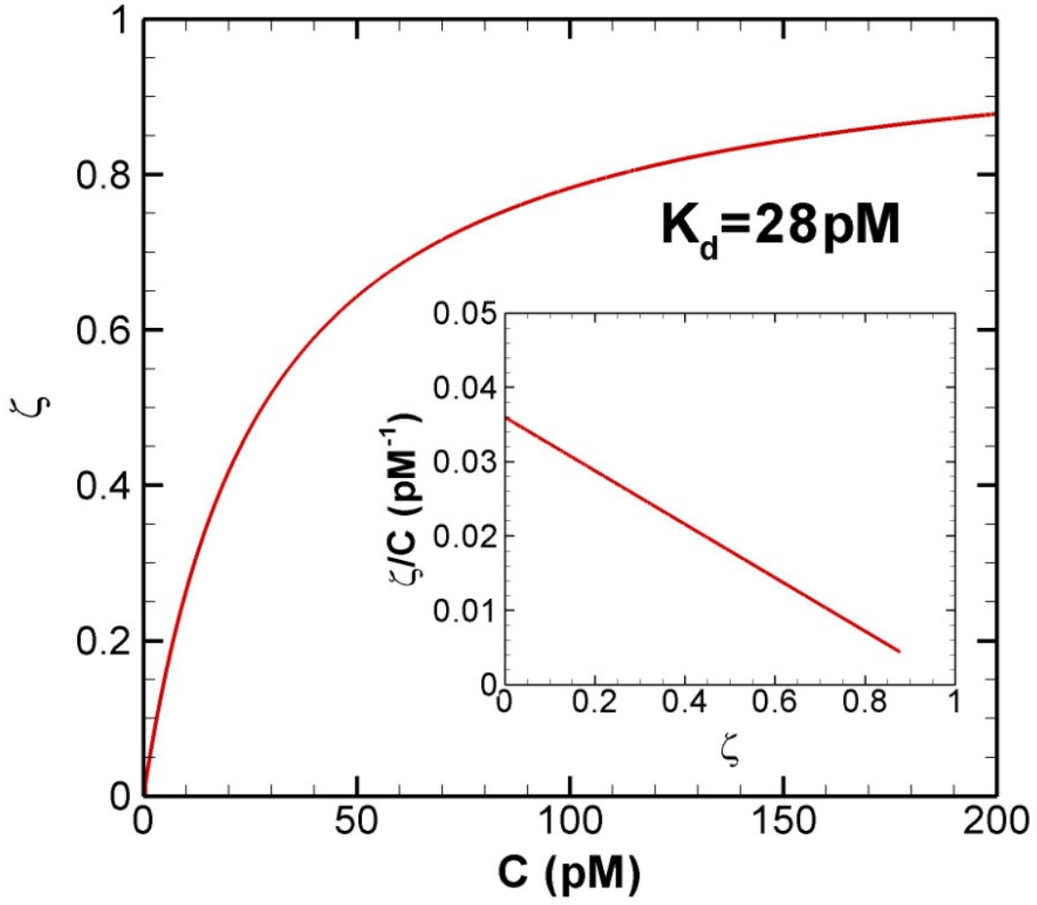

In vitro experiment

Muro *et al.* J. Pharmacol. Exp. Ther. 317 1161 (2006)

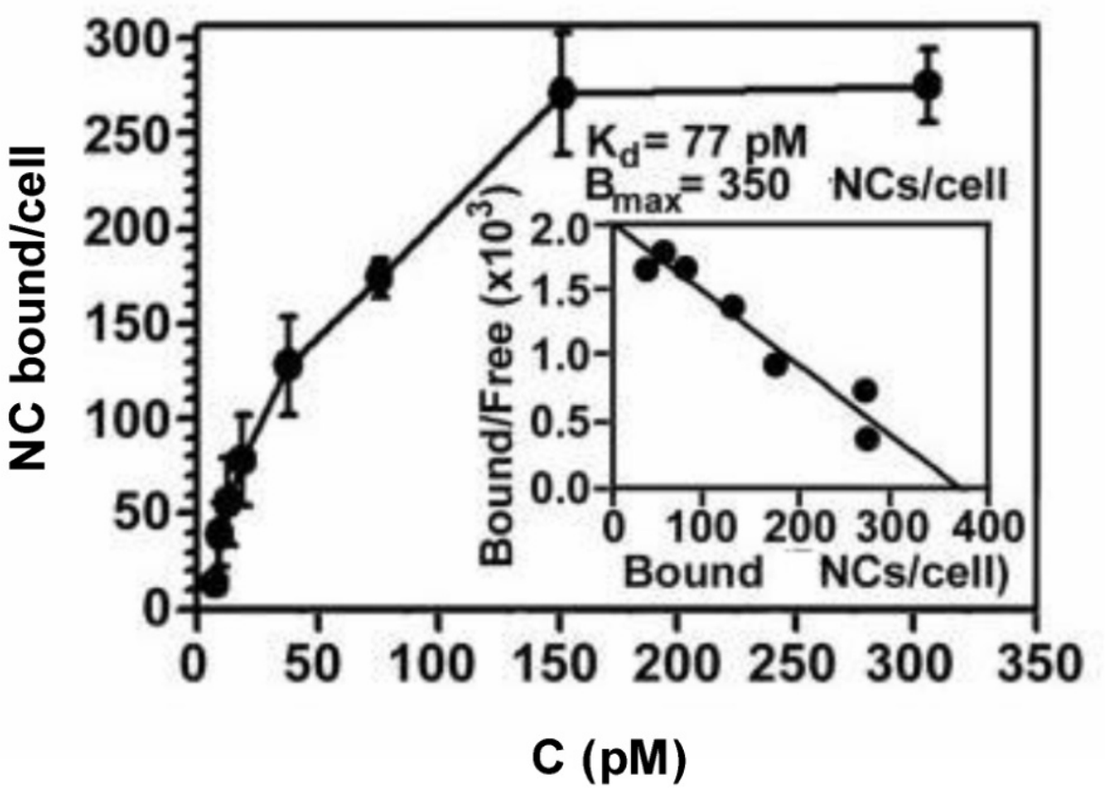

According to Langmuir binding model, the fractional binding:

$$\zeta = \frac{C/K_d}{1 + C/K_d} \qquad K_d = 1/K_a$$

Liu *et al.* (2010) *PNAS* **107** 16530-16535

K_d	Model (27°C)	Experiment (4°C)
R6.5-ICAM-1	3.2nM	8.5nM
NC-cell	28pM	77pM

Zero-fit model predictions are consistent with in vitro cellular experiments

Effect of Flow on NC Adhesion: Shear Enhanced Binding and Rolling Behavior

J. Liu, et al., Biophys J, 2011

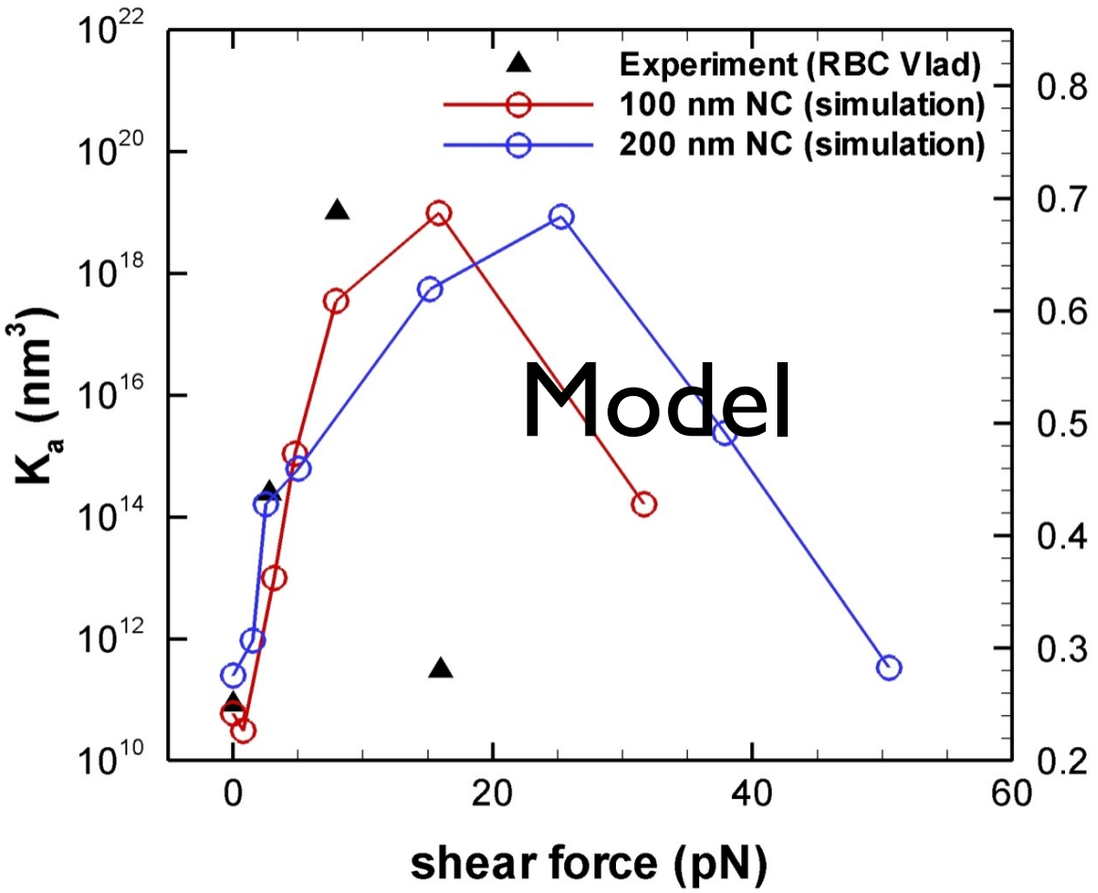

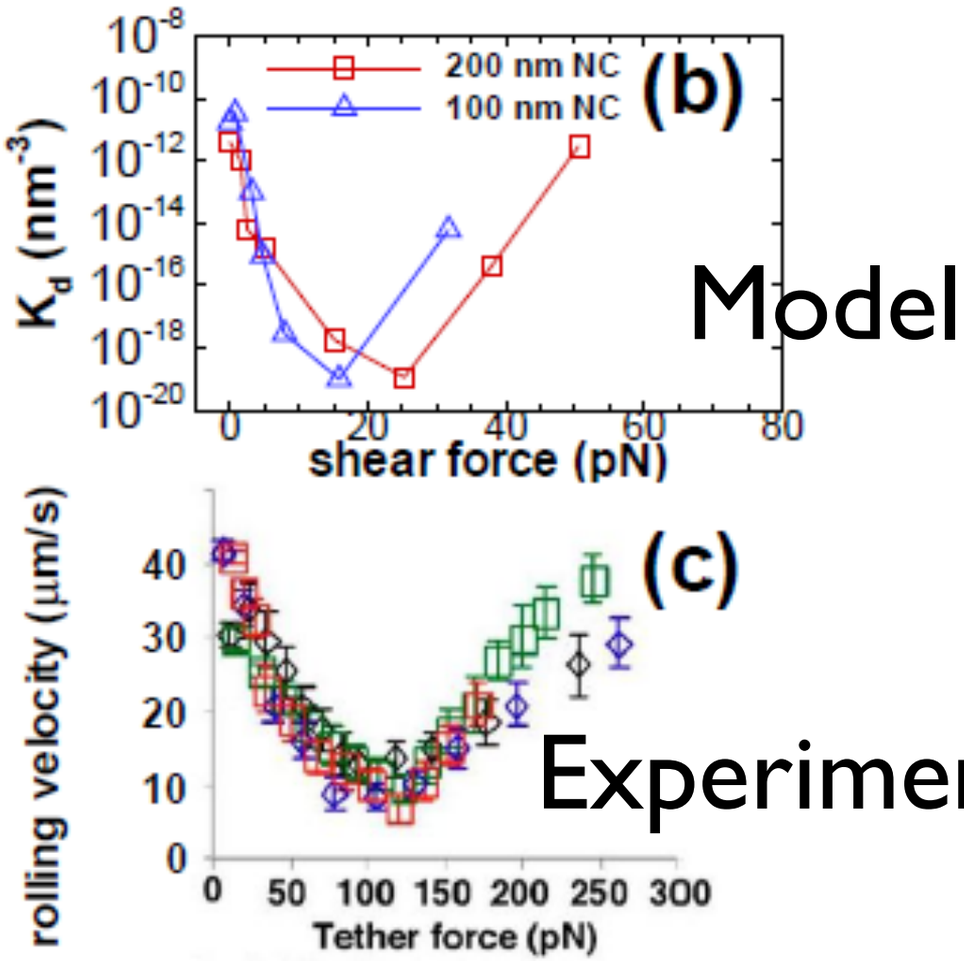

Model predicts shear-thresholding even without catch bonds

Effect of Nanocarrier Surface Coverage σ_s (# antibodies per NC)

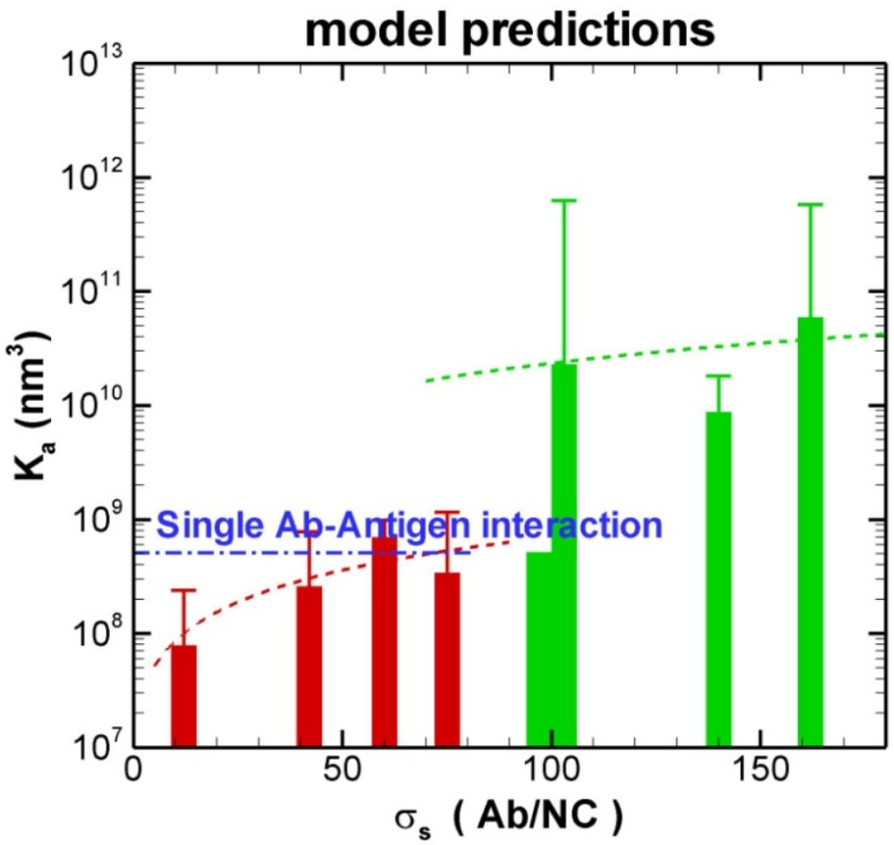

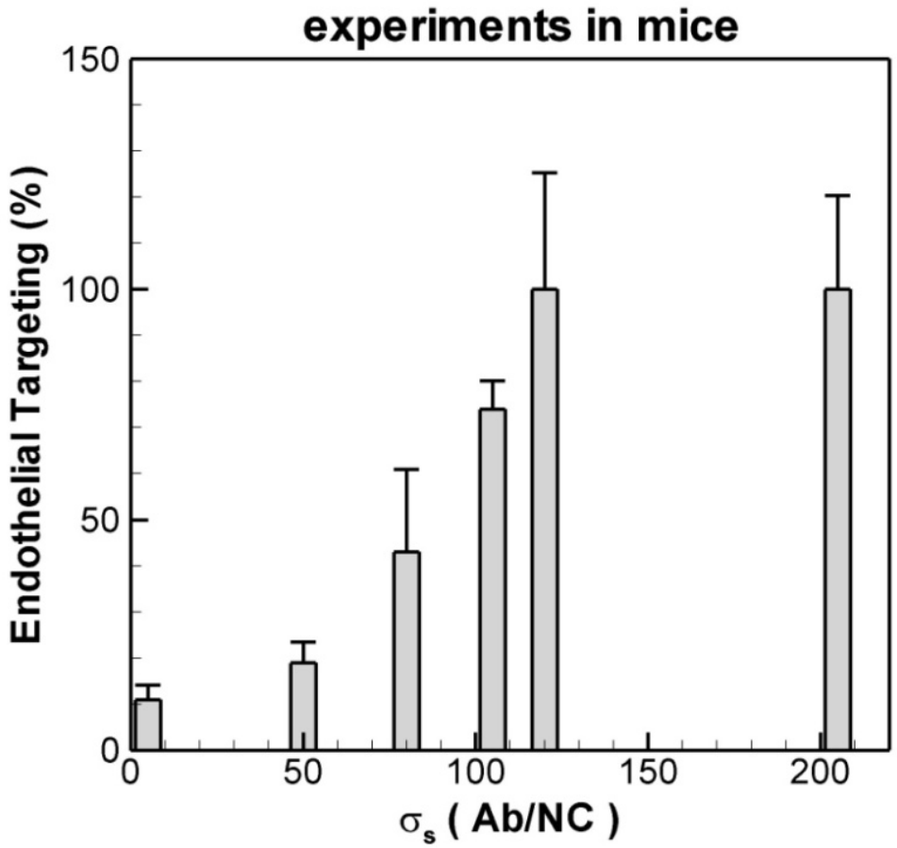

- A threshold at σ_s ~45% (100Ab/NC), the binding affinity abruptly drops below that of single antibody to antigen

Liu *et al.* (2010) *PNAS* **107** 16530-16535

$$K_a = \frac{(N_{ab}/N_b)\Delta\omega}{8\pi^2} \times \frac{A_{R,b}^{(1)} \times A_{R,b}^{(2)} \times \ldots \times A_{R,b}^{(N_b)}}{A_{R,ub}^{(1)} \times A_{R,ub}^{(2)} \times \ldots \times A_{R,ub}^{(N_b)}} \times A_{NC,b} \int e^{-\beta W(z)} dz$$

- Linear dependence below and above the threshold at fixed multivalency, dotted lines.
- Exponential reduction because of the multivalency change (from 3 to 2) around σ_s ~45%

Model predictions are consistent with results of in vivo mice experiments

Tissue Selectivity Predictions

Zern, ACS Nano, 2013

Modeling Prediction

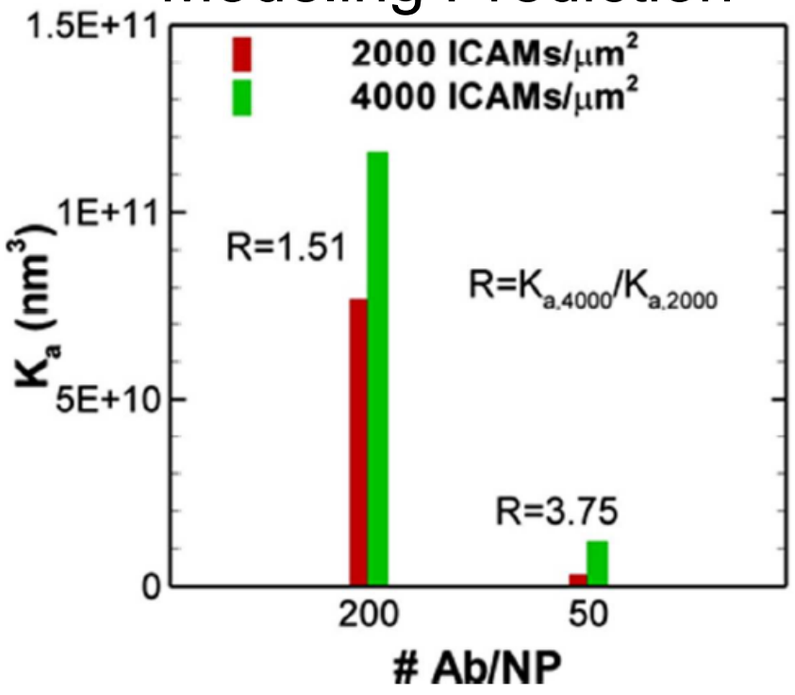

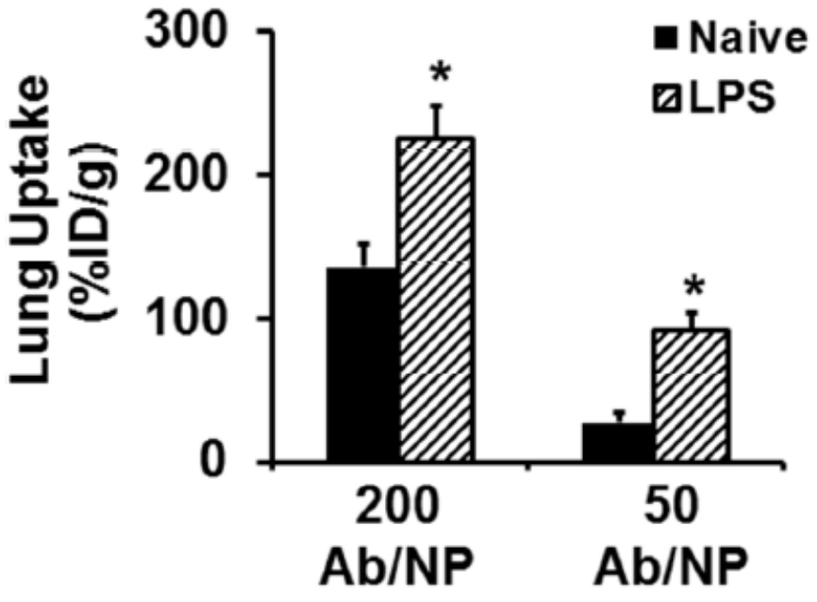

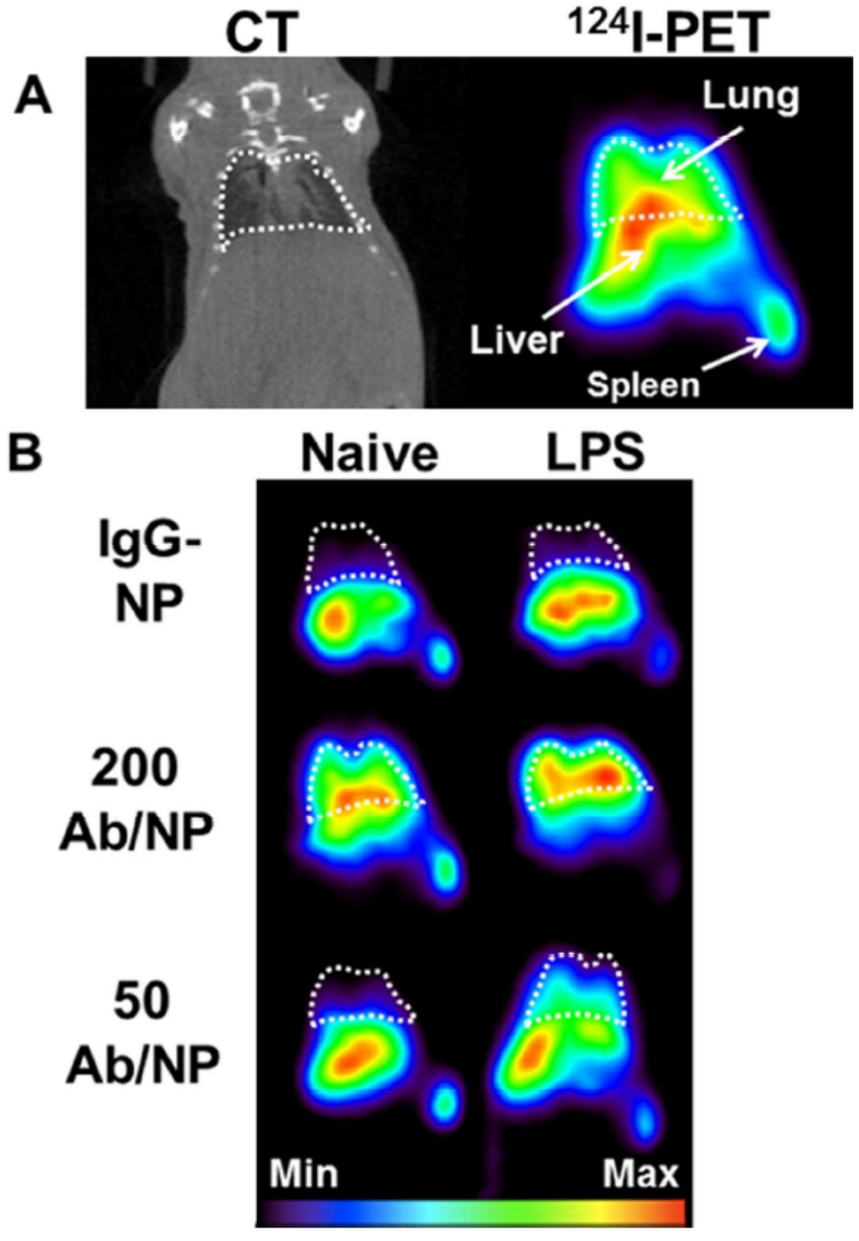

Reduction of nanoparticle avidity enhances the selectivity of vascular targeting and PET detection of pulmonary inflammation

Targeting Live Cells: Role of Cell Membrane Undulations in Nanocarrier Adhesion

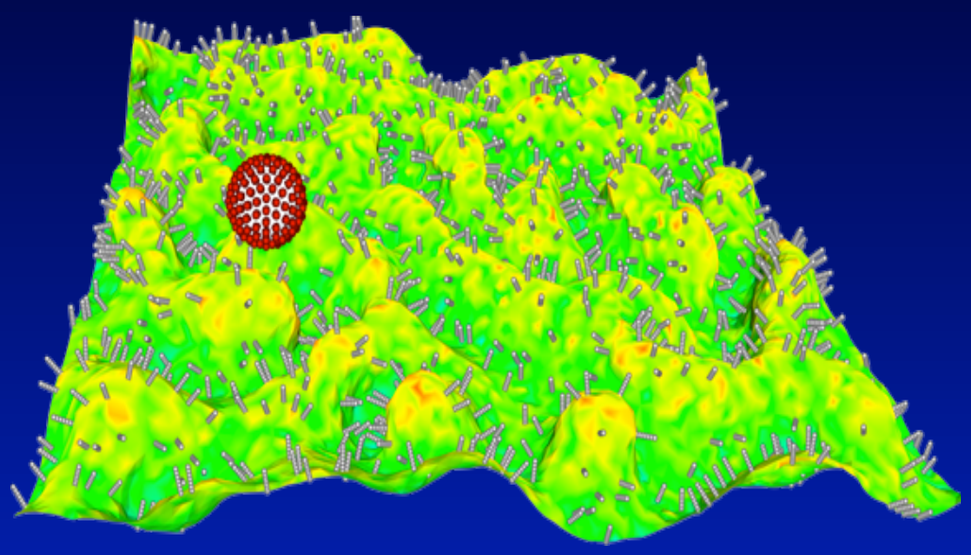

Undulating membrane is modeled as a thin, elastic, fluid surface with energy

$$\mathscr{H}_{\mathrm{mem}} = \int \frac{\kappa}{2} \left(2H - C_0\right)^2 ds$$

Bending rigidity

Mean curvature

Spontaneous curvature

Membrane undulations are simulated using dynamically triangulated Monte Carlo.

- Membrane Fluidity impacts Targeting
- Intracellular Signaling impacts Targeting
- Carrier Internalization is coupled to Targeting

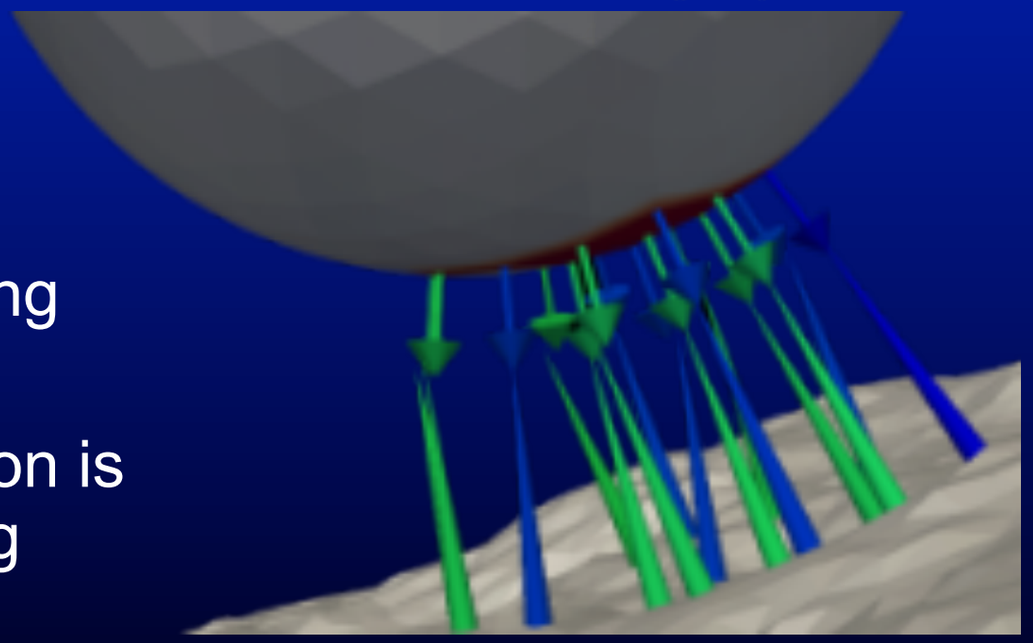

Membrane Properties

(a) Bending rigidity

(b) Surface tension

(c) Excess surface area

Our model quantifies how membrane mobility and surface curvature affect nanocarrier (NC) binding

Effect of Excess Membrane Area and Undulations on Multivalency

larger excess area $\kappa = 20k_BT$ smaller excess area

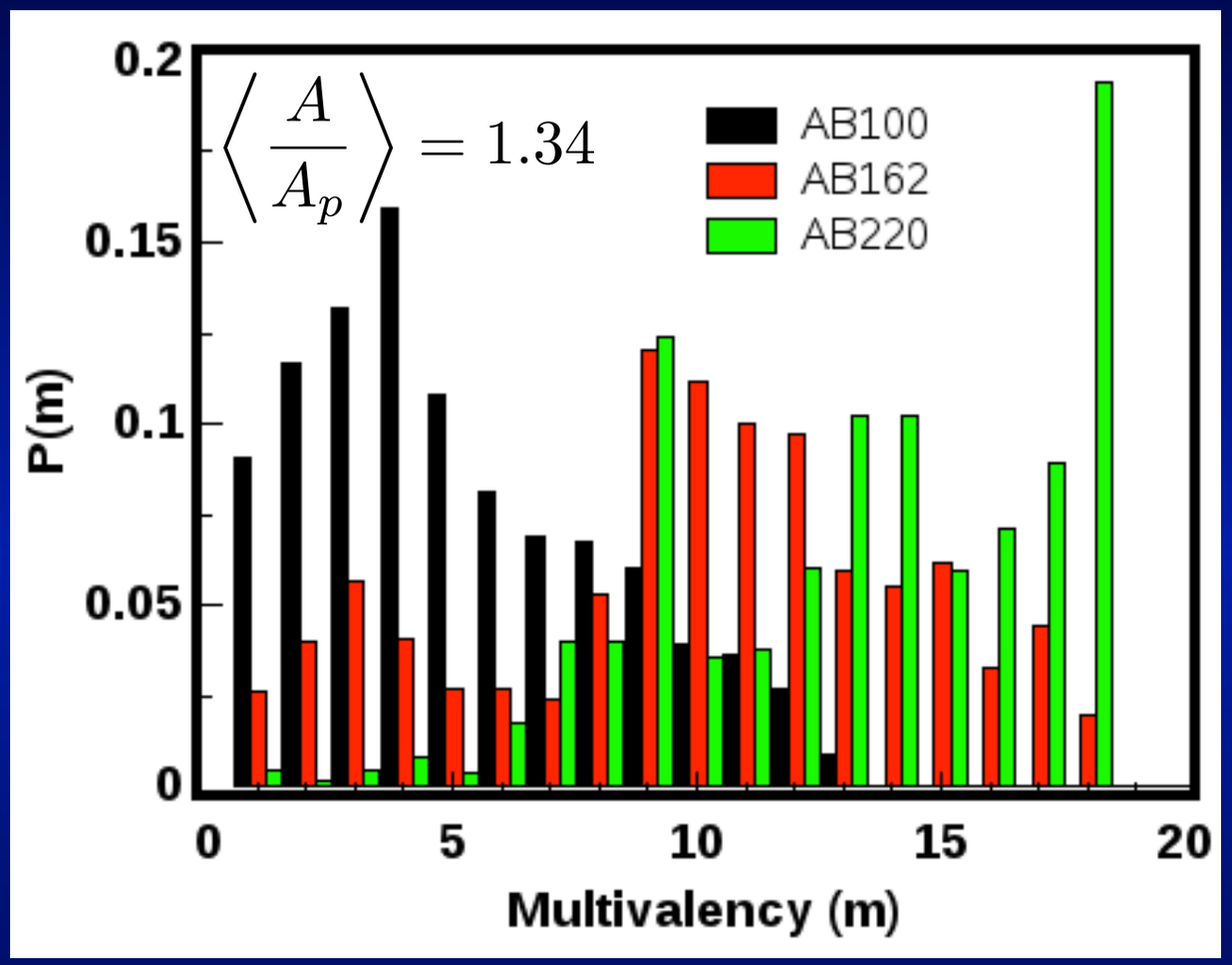

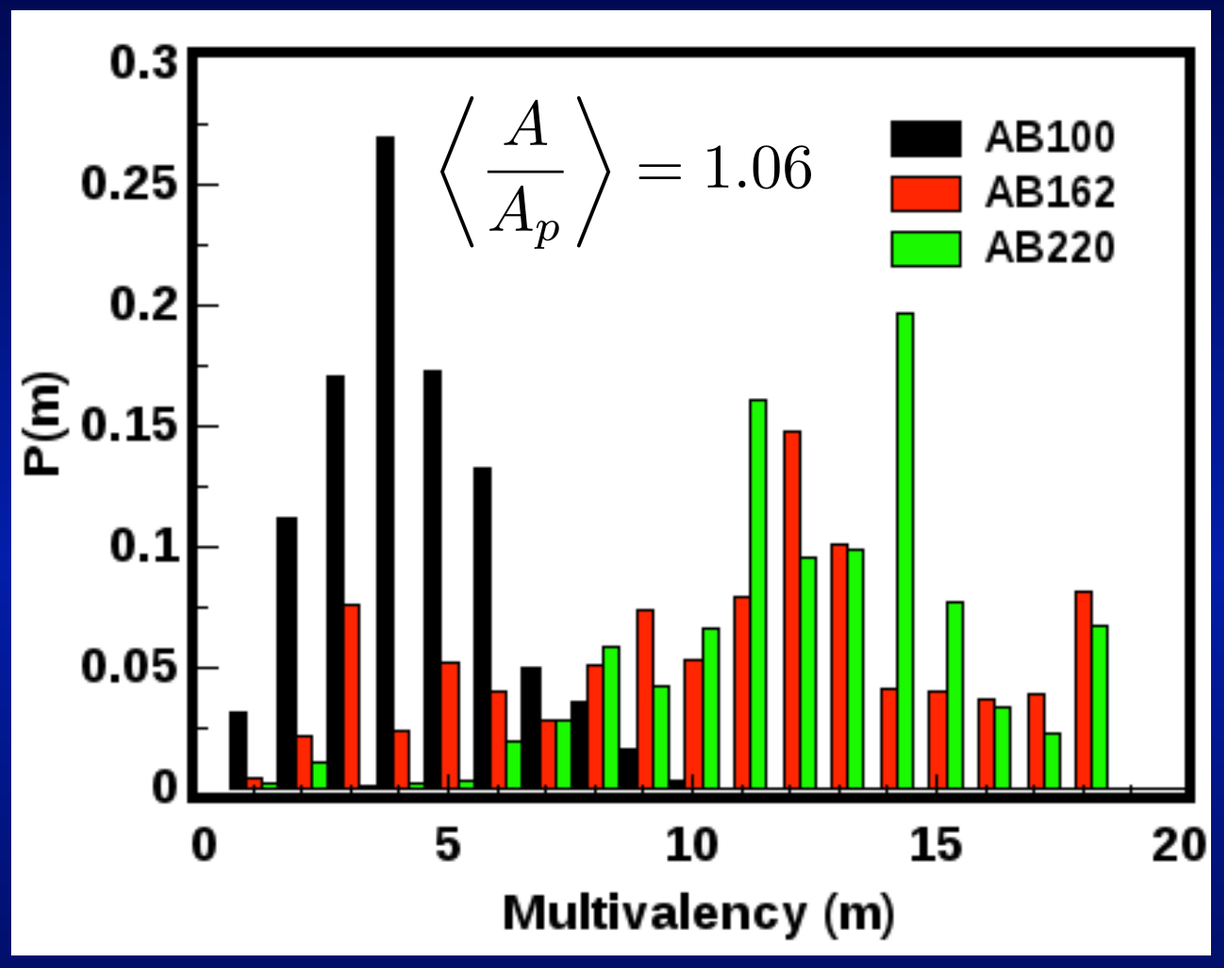

Excess surface area in the membrane promotes higher multivalent binding

Presence of excess membrane area can significantly impact nanocarrier binding to the cell membrane and can promote wrapping of cargo which is extremely important in uptake of nanocarriers by cells.

Polyvalent Interactions Between NC and Live Cells in Flow

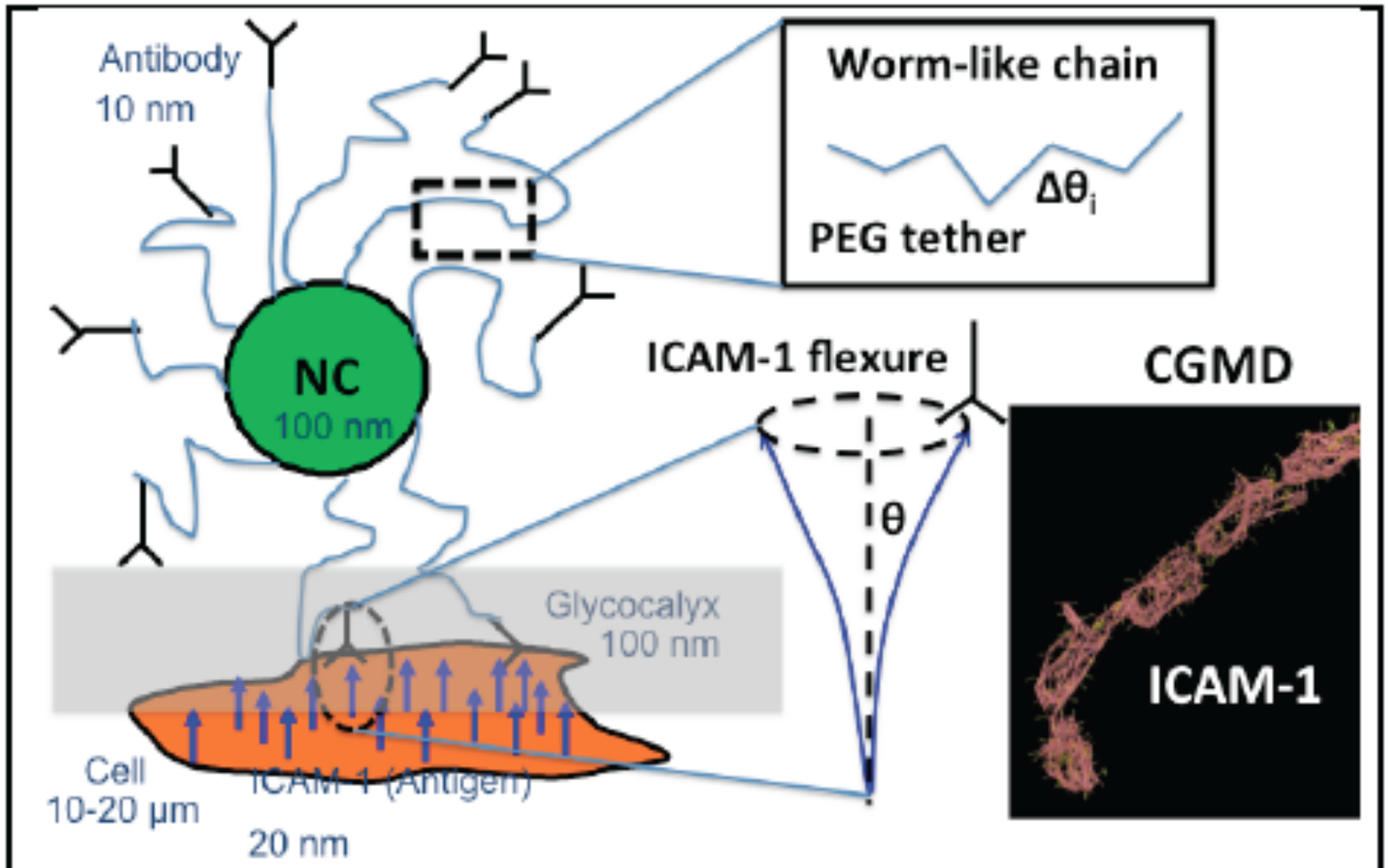

Fig. 10: Multiscale model for NC adhesion interactions with molecular specificity

$$E[\theta(s)] = \sum_{i=1}^{N} \frac{\xi_P (\Delta\theta_i)^2 k_B T}{2\Delta s} + \vec{f}_i \cdot \overrightarrow{\Delta r_i} + \vec{T}_i \cdot \overrightarrow{\Delta\psi_i},$$

Next-Generation Pharmacodynamic Models in Personalized Medicine

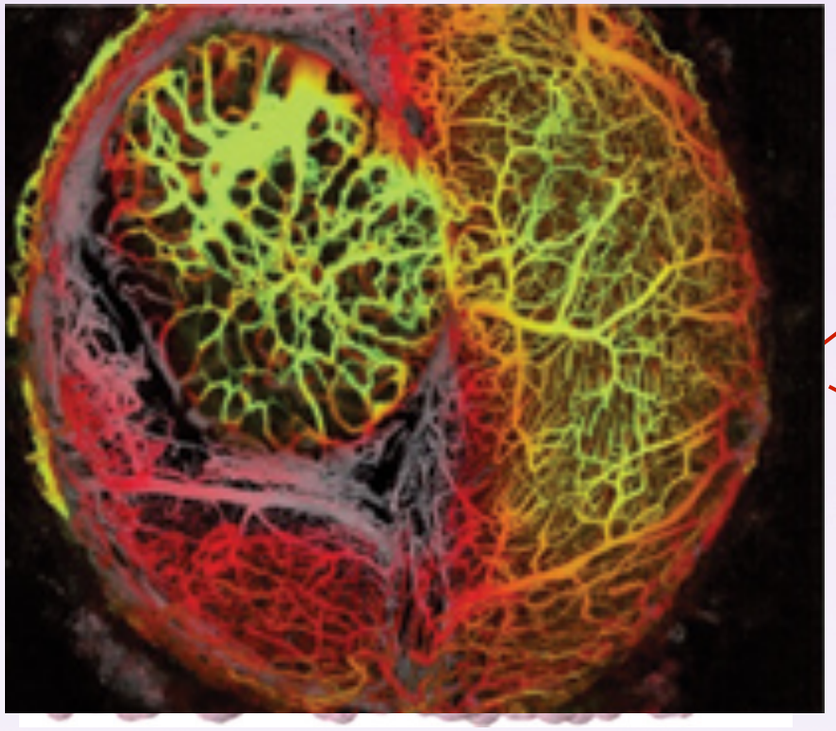

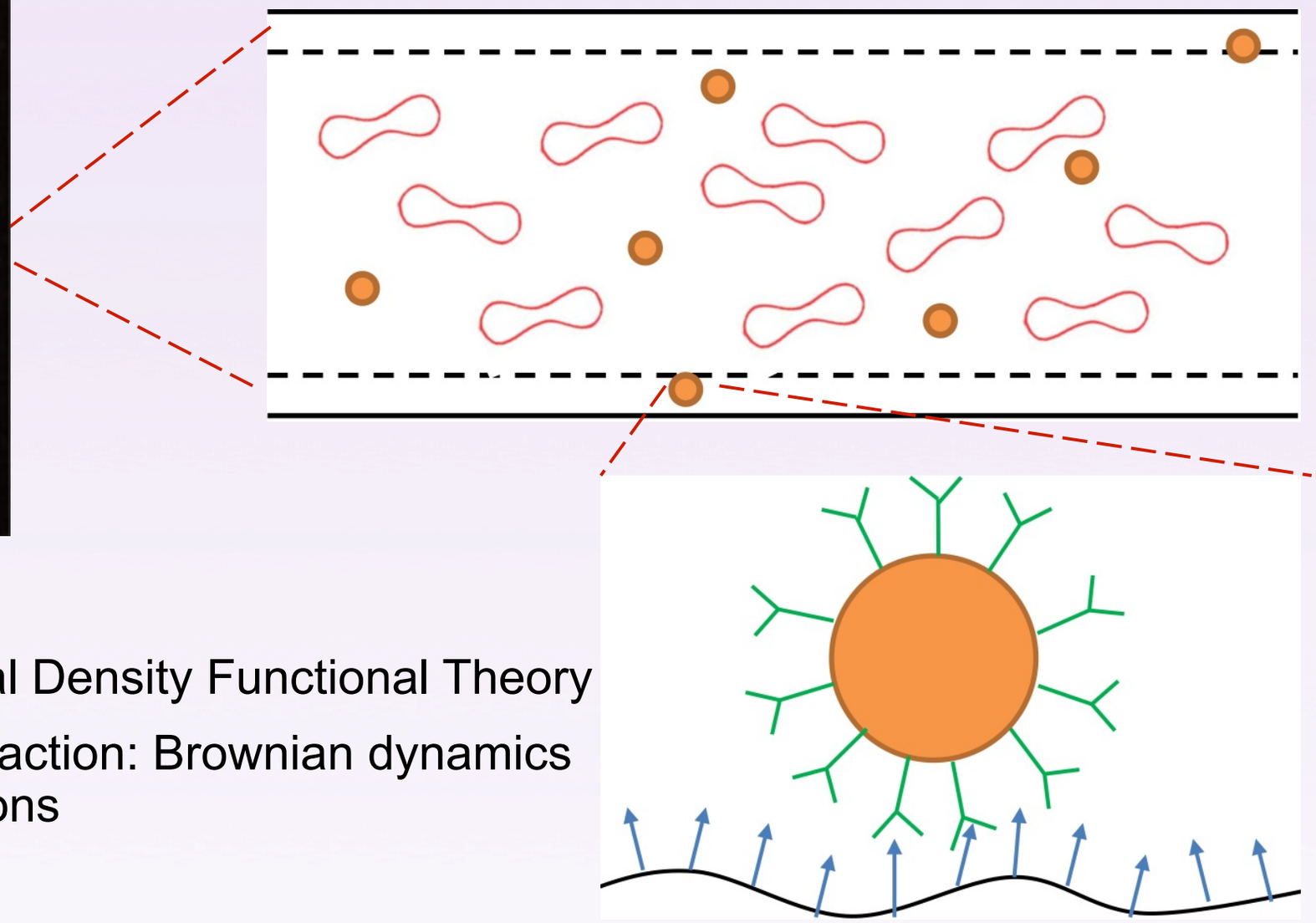

Nanoscale Hydrodynamics

- Mean-field models: Dynamical Density Functional Theory
- Rigorous Hydrodynamic Interaction: Brownian dynamics and direct numerical simulations

Nanoscale Adhesion

- Generalized Langevin equations for NC binding and tethering relaxation
- Direct parameterization using single molecule experiments or microscopic simulations

How do hydrodynamic interactions, Brownian forces, and ligand-receptor relaxations affect the Nanocarrier adhesion

Objective: To develop easily computable yet physiologically ***predictive next-generation pharmacodynamic models*** for targeted drug delivery to treat scales ranging from vasculature hydrodynamics to ligand-receptor mediated NC adhesion at organ scale

Generalized Langevin Dynamics for Functionalized Nanocarrier Adhesion to Cell Surfaces in the Presence of Hydrodynamic Interactions

Fluid Dynamics of Targeted Drug Delivery

Microscale Transport

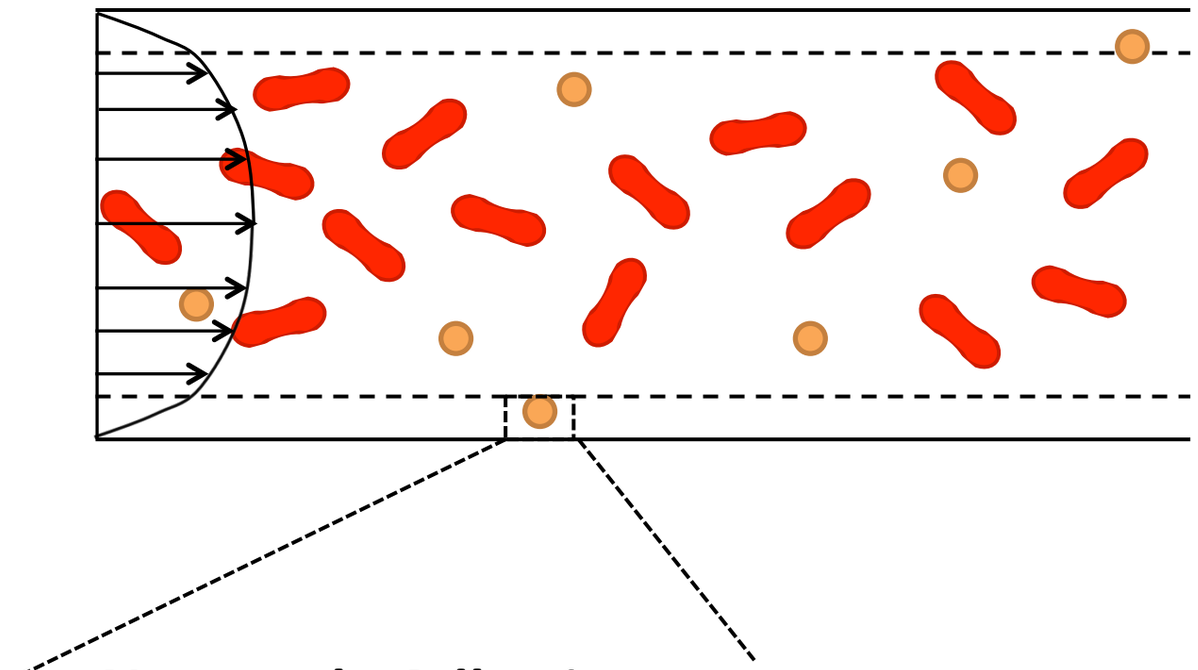

- Margination of "smaller particles" predicted by hydrodynamic simulations:
  Crowl and Fogelson, *J. Fluid Mech.*, 2011
  Zhao and Sheqfeh, *Phys. Rev. E*, 2011
  Tan et al., *Soft Matter*, 2012
  Kumar and Graham, *Phys. Rev. Lett.*, 2012
- Length scales for TDD:
  20 ~ 50 µm vessels
  1 ~ 8 µm blood cells
  100 nm ~ 1 µm nanocarriers

Nanoscale Adhesion

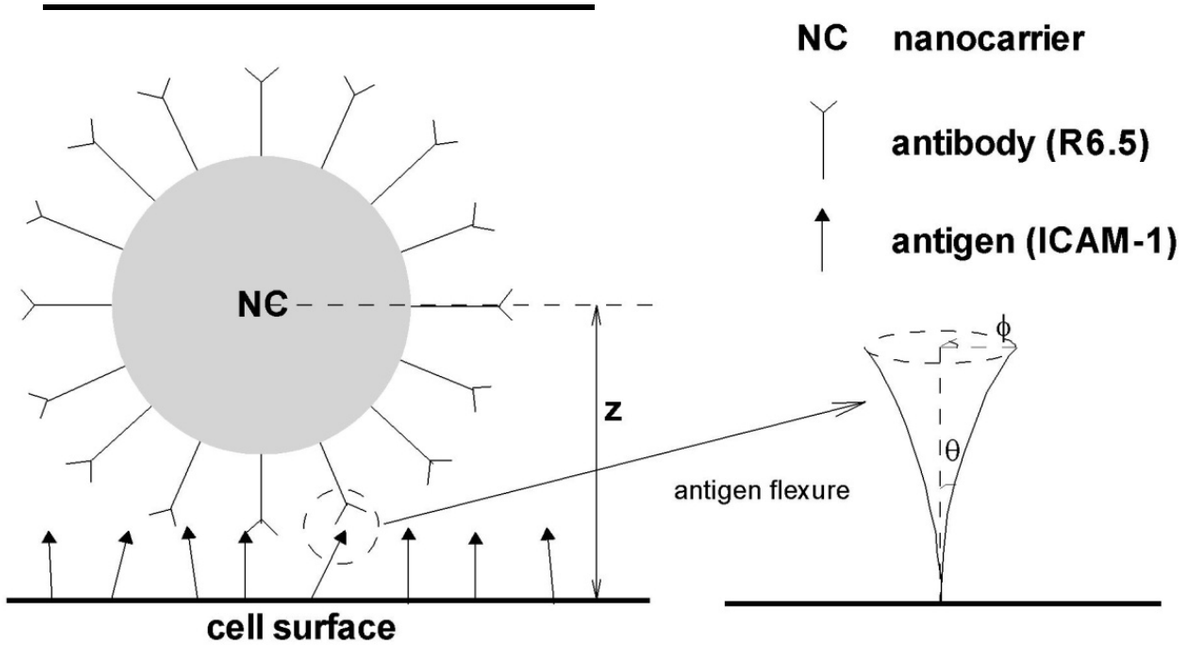

- Binding affinity predicted by Monte Carlo simulations validated *in vivo* and *in vitro*:
  Jin et al., *PNAS*, 2010
- Length scales for TDD:
  100 nm ~ 1 µm nanocarriers
  15 ~ 20 nm ligands and receptors

Challenge: How can we bridge the hydrodynamic and adhesion length scales in a tractable computational model?

Fast and Easily Computable Approach for Multiscale Bridging of NC Hydrodynamics and Adhesion

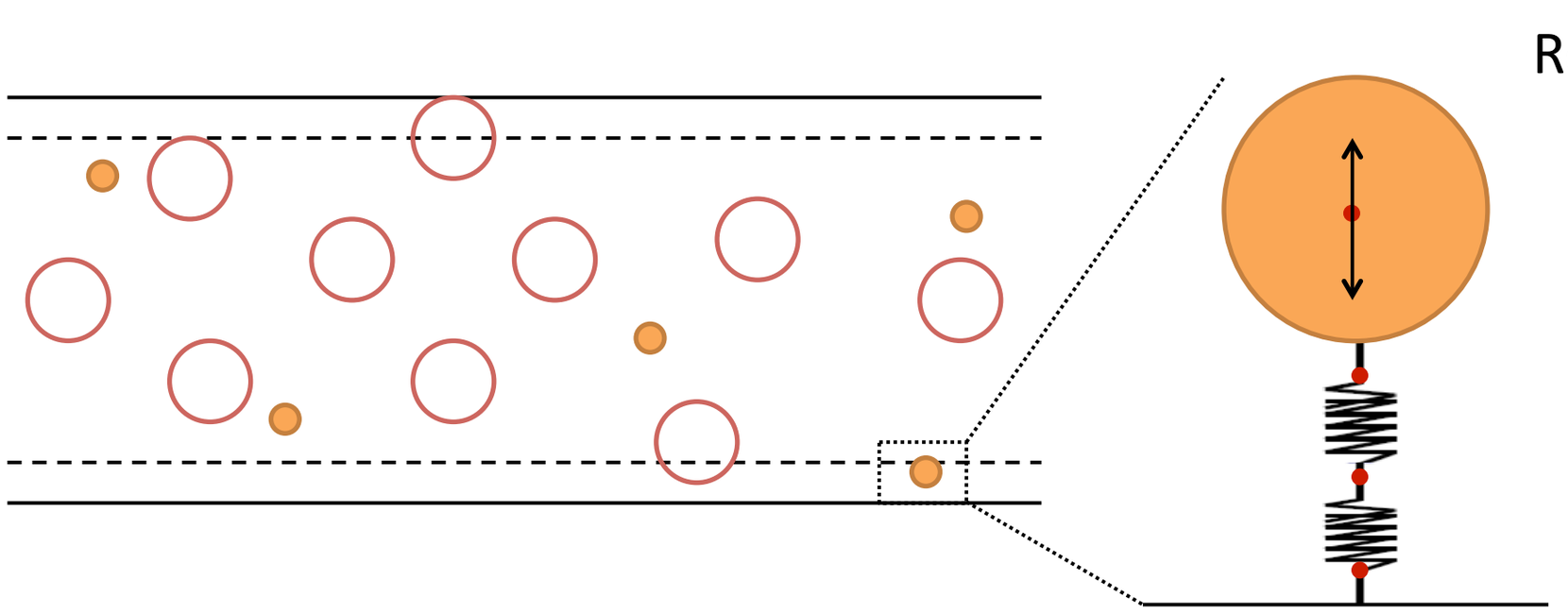

Red blood cells (RBC):

Nanocarriers (NC):

Incorporate RBC-driven margination effect for more transparent clinical design

Dynamic density-functional theory for RBC cross-vessel distribution

$$\rho_{RBC}(\mathbf{r}') \qquad \Phi_{RBC}(\mathbf{r}) = \int_V \rho_{RBC}(\mathbf{r}')\langle\phi\rangle_1(\mathbf{r},\mathbf{r}')d\mathbf{r}'$$

Mean-field approach

Incorporate transient dynamics of NC for in the presence of receptor protein relaxation

Generalized Langevin equations for NC-endothelium adhesive dynamics

$$C_v(t) = \frac{\langle U(t)U(0)\rangle}{(k_BT/m_p)} \qquad C_x(t) = \frac{\langle \delta x(t)\delta x(0)\rangle}{\delta x(0)^2} \qquad P(x)$$

Velocity autocorrelation

Position autocorrelation

Position probability distribution

Thermodynamic Perspective of RBC Distribution

Complex blood flow

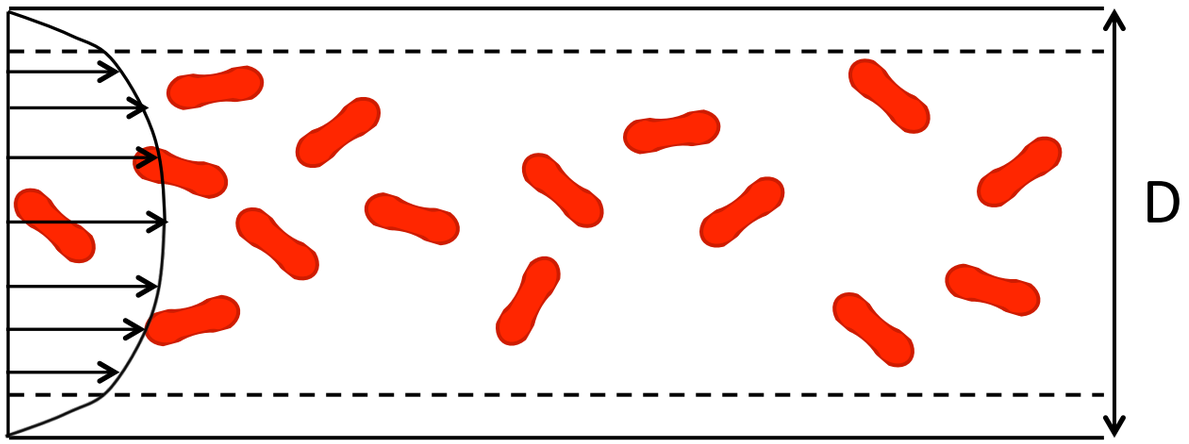

Data for arterioles and venules

Vessel diameter: D (μm) [1]	20–50
Average velocity: U_{av} (cm/s) [1]	0.2–5
RBC hematocrit: H_{ct} [2]	0.2–0.3
Relative viscosity: $\mu_{rel}=\mu/\mu_{plasma}$ [3]	1.5–1.8

[1] Mazumdar, *Biofluid Mechanics*, 2004
[2] Oshima et al., *Curr. Pharm. Biotechnol.*, 2012
[3] Pries et al, *Circ. Rec.*, 1994

Effective hard-sphere-like RBC model

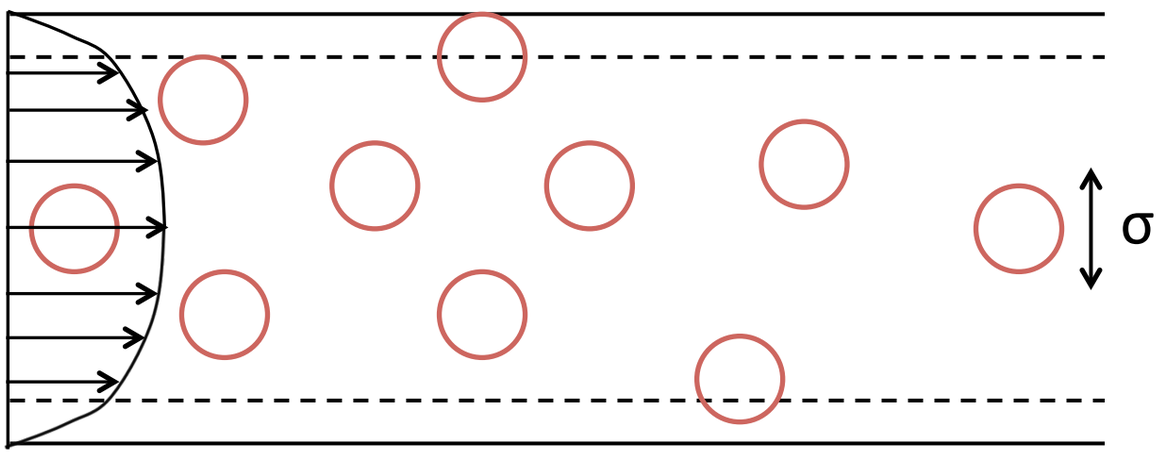

Data for hard sphere suspension

Volume fraction: ϕ_b [4]	0.15–0.2
Cell diameter: σ (μm)	4.3–5.2
D/σ	3.8–11.6

[4] Batchelor and Green, *J. Fluid Mech.*, 1972

$$\mu_{rel} = 1 + 2.5\phi_b + 7.6\phi_b^2$$

The physiological data summarized here provide a consistent and unambiguous scheme to define the parameters of our model without any additional fitting

Dynamic Density-Functional Theory (DDFT) for a Hard-Sphere Model

N-particle Smoluchowski equation

$$\frac{\partial P_N}{\partial t} + \nabla \cdot \mathbf{j}_N = 0 \qquad \mathbf{j}_N = \mathbf{U} P_N + \frac{\mathbf{D}}{k_B T} \cdot \left(\mathbf{F}^P - k_B T \nabla \ln P_N \right) P_N$$

Averaging over configuration of N-1 particles (mean-field model)

$$\frac{\partial \rho(\mathbf{r},t)}{\partial t} + \nabla \cdot \left[\rho(\mathbf{r},t) \langle \mathbf{U} \rangle_1 (\mathbf{r},t) \right] = \nabla \cdot \left[\frac{\langle \mathbf{D} \rangle_1 (\mathbf{r})}{k_B T} \cdot \rho(\mathbf{r},t) \nabla \frac{\delta \Omega[\rho(\mathbf{r},t)]}{\delta \rho(\mathbf{r},t)} \right]$$

$$\langle \mathbf{U} \rangle_1 = \langle \mathbf{U}^0 \rangle_1 + \langle \mathbf{U}' \rangle_1$$

D: diffusivity tensor
Ω: Grand potential
$\langle \mathbf{U}^0 \rangle_1$: average flow field set up by N-1 particles
$\langle \mathbf{U}' \rangle_1$: perturbation due to Nth particle

(1) Equilibrium grand potential functional
(2) "Hydrodynamically dilute" for motion of test particle given an average flow field
(3) $\rho=\rho_b$ w/o V_{ext} and $\langle f_1 \rangle_1$ Symmetric U(r) and ρ(r)

Particle migration due to inertial lift

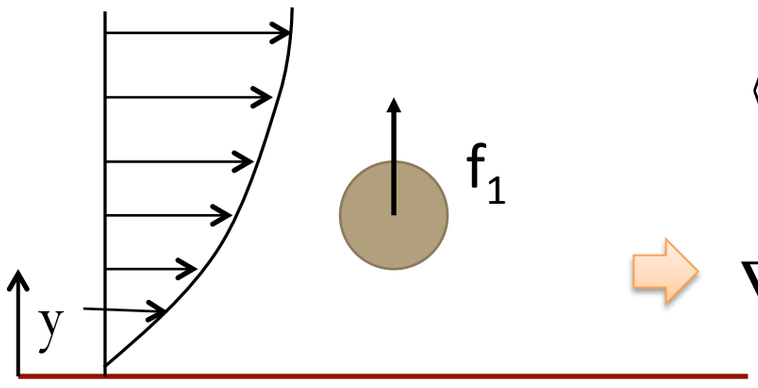

$$\langle \mathbf{U}' \rangle_1 = \frac{D_0^\perp}{k_B T} \langle \mathbf{f}_1 \rangle_1$$

$$\Rightarrow \quad \nabla \cdot \left[\rho(\mathbf{r}) \langle \mathbf{U}' \rangle_1 (\mathbf{r}) \right] = \nabla \cdot \left[\frac{D_0^\perp}{k_B T} \rho(\mathbf{r}) \nabla \frac{\delta \Omega[\rho(\mathbf{r})]}{\delta \rho(\mathbf{r})} \right]$$

Steady-state particle distribution predicted from DDFT

$$\rho(\mathbf{r}) = \rho_b \exp\left\{ c^{(1)}(\mathbf{r}) - c_b^{(1)} - \frac{V_{ext}(\mathbf{r})}{k_B T} + \int_0^r \frac{\langle f_1 \rangle_1 (r')}{k_B T} \mathrm{d}r' \right\}$$

$$c^{(1)}(\mathbf{r}) = -\frac{1}{k_B T} \frac{\delta F_{ex}[\rho(\mathbf{r})]}{\delta \rho(\mathbf{r})} \qquad c_b^{(1)} = -\frac{1}{k_B T} \frac{\partial F_{ex}(\rho_b)}{\partial \rho_b}$$

-- Excess energy from smoothed density approx. by Tarazona (1985)
-- Wall acts as external potential
-- Hydrodynamic effect captured by work done by the lift force

Effect of Flow and Confinement: DDFT Predicts Flow-Dependent Cell Migration

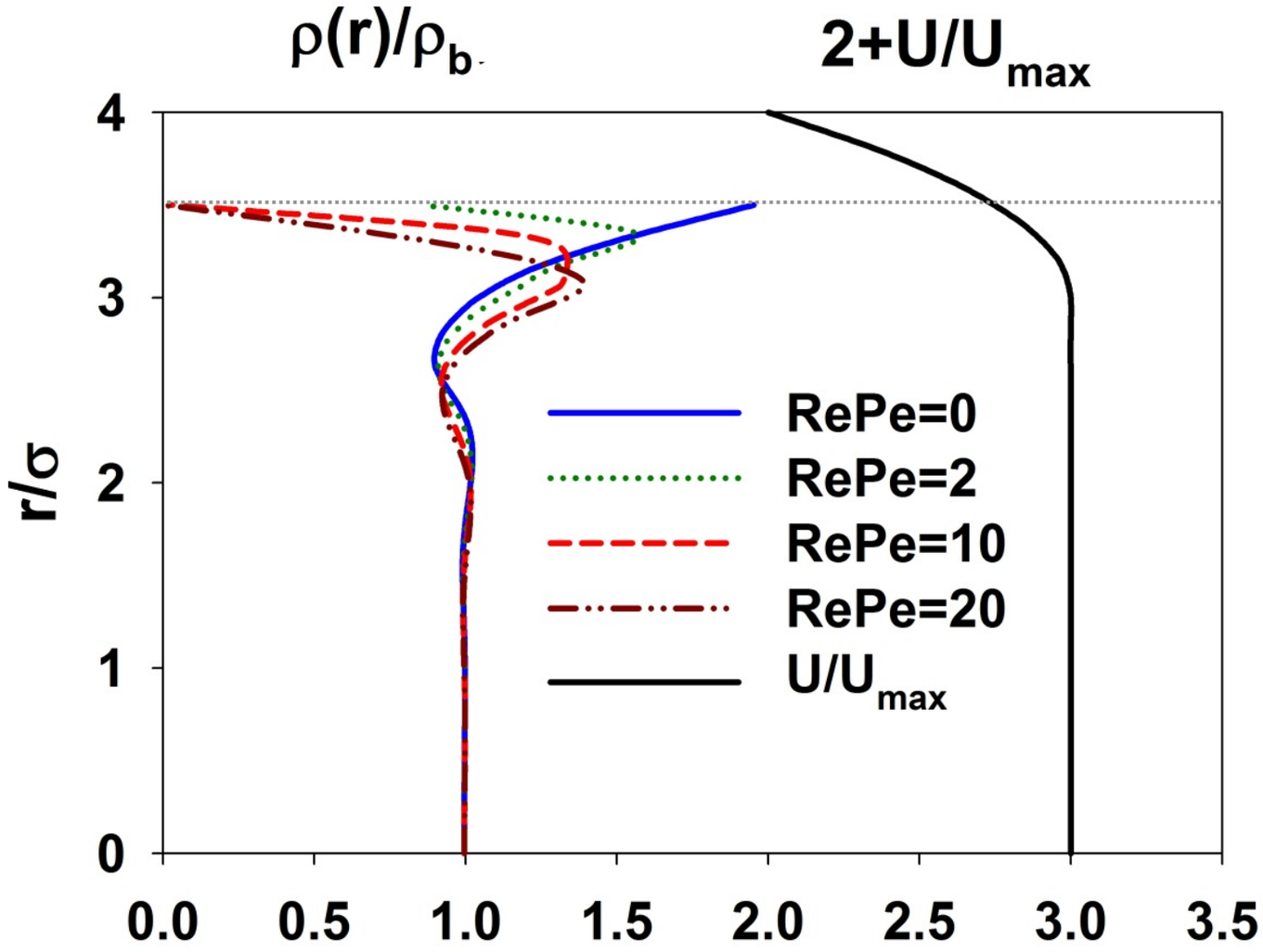

$L=\sigma$; $R_c=4\sigma$; $\phi_b=0.15$

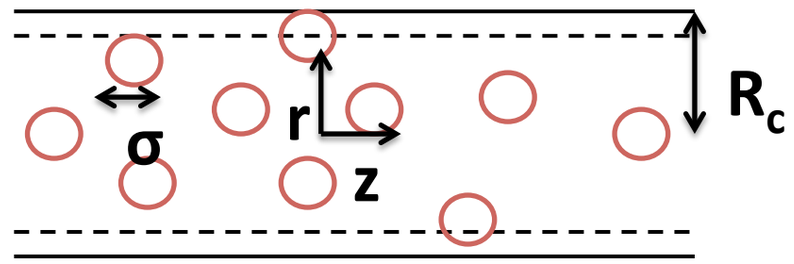

For larger flow rates, particle distribution shows a "depletion layer" consistent with the average flow profile

$$\rho_{RBC}(\mathbf{r}') \Rightarrow \Phi_{RBC}(\mathbf{r}) = \int_V \rho_{RBC}(\mathbf{r}')\langle\phi\rangle_1(\mathbf{r},\mathbf{r}')d\mathbf{r}'$$

$$-\nabla\Phi_{RBC}$$

Extension of HS model to disc or ellipsoidal shaped particles can be achieved either by suitable DDFT closure application for anisotropic particles or through Monte Carlo Simulations

NC Adhesive Dynamics with Receptor Protein Frictional Relaxation

1D Generalized Langevin Dynamics for an engineering model

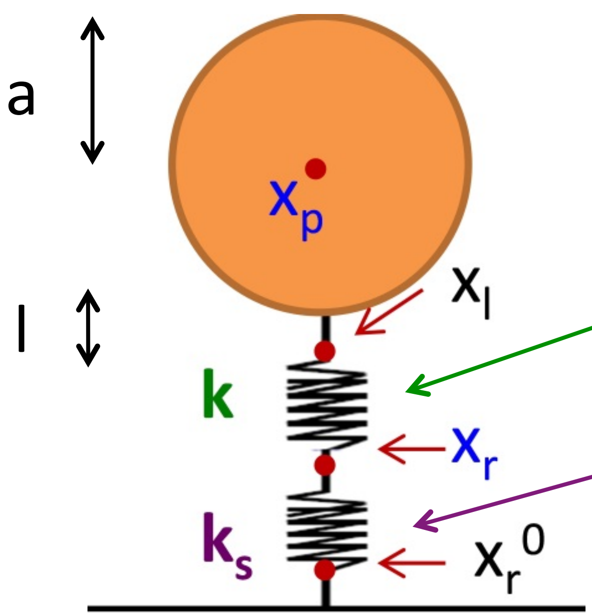

Hookean springs model potential forces

receptor-antibody interaction

receptor protein dynamics

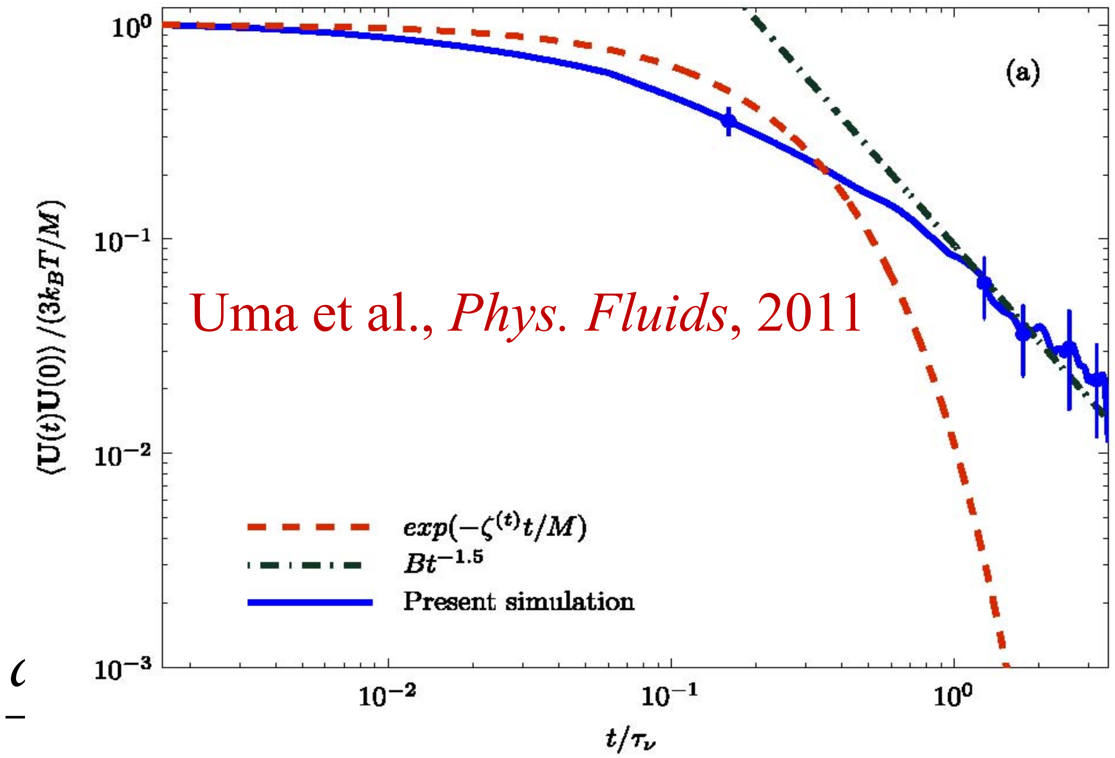

NC translation

$$m_p \frac{d^2 \bar{x}_p(t)}{dt^2} = -\int_{-\infty}^{t} \zeta_p^{(trans)}(t-t') \frac{d}{dt} \ldots$$

$$\zeta_p^{(trans)}(t-t') = \zeta_{p,0}(\lambda_p)|t-t'|^{-\lambda_p}$$

Receptor relaxation

$$0 = -\int_{-\infty}^{t} \zeta_r^{(trans)}(t-t') \frac{dx}{dt'} dt' - (k + k \ldots$$

$$\zeta_r^{(trans)}(t-t') = \zeta_{r,0}(\lambda_r)|t-t'|^{-\lambda_r}$$

Power-law memory kernel satisfying fluc

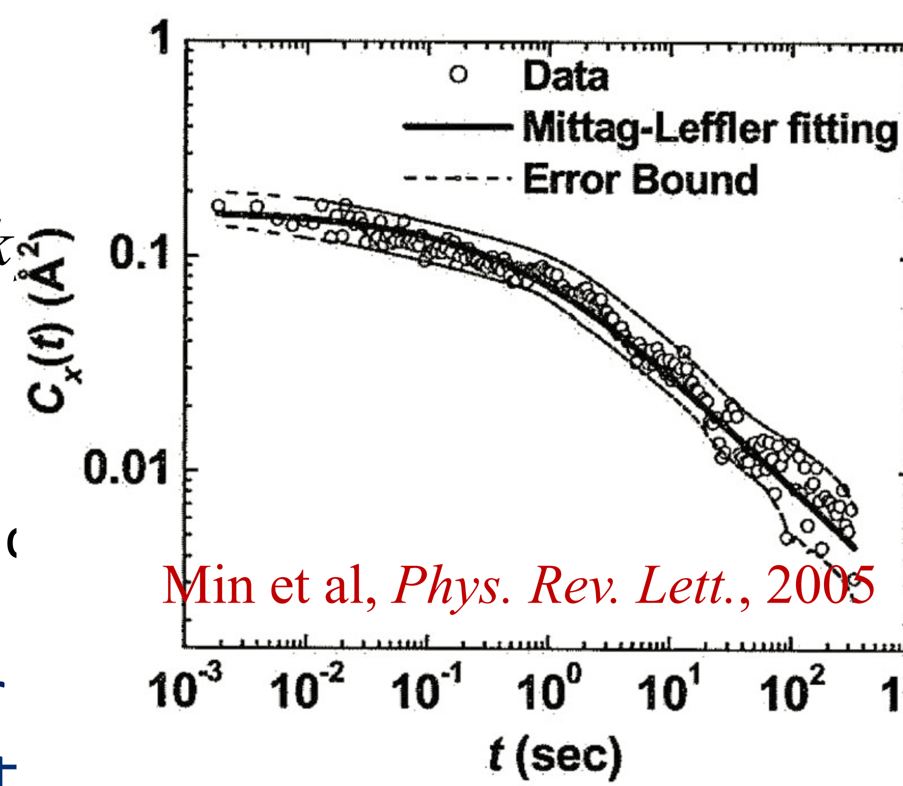

NC monovalently attached through a single receptor

Extension to multivalent binding: 1D→3D models; at... ...el

Velocity Autocorrelation Function vs. Position Fluctuation Autocorrelation Function

Velocity Autocorrelation of NC

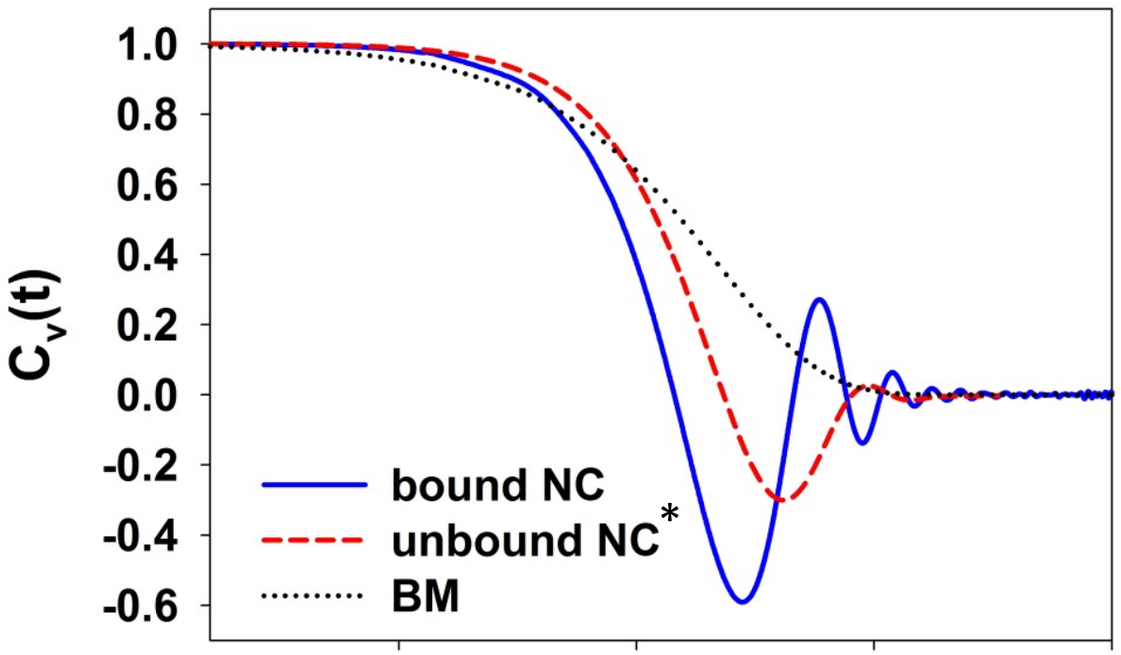

Position Autocorrelation of NC/receptor

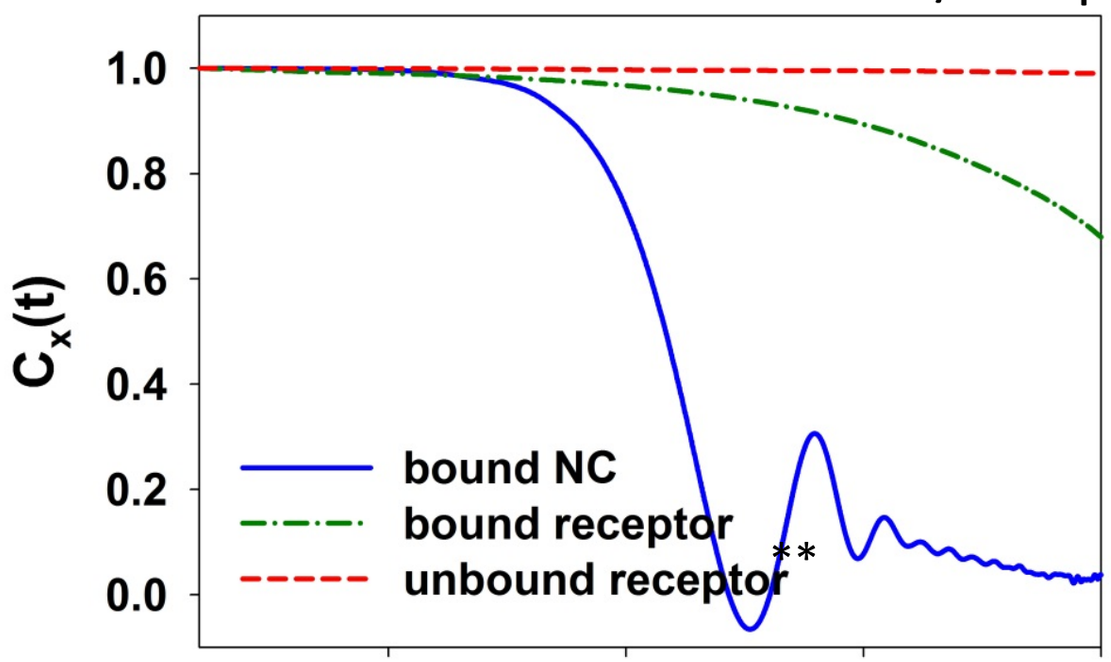

a=250 nm
k=1 N/m [1]

$\lambda_p = \lambda_r = 0.5$
k_s=1.882 N/m [2]
$\zeta_{r,0}/k_s$=0.7 $s^{0.5}$ [2]
$\zeta_{r,0}/\zeta_{p,0}$=2.2x10^4

Analytical* result for VACF of free NC in unbounded space:

$$C_v(t) = \frac{\langle U(t)U(0)\rangle}{(k_B T/m_p)} = E_{2-\lambda_p}\left[-\zeta_{p,0}(\lambda_p)\frac{\Gamma(1-\lambda_p)}{m_p}t^{2-\lambda_p}\right] \qquad \zeta_{p,0}(\lambda_p) = \frac{6\pi m_p}{\Gamma(1-\lambda_p)}\left(\frac{\mu a}{m_p}\right)^{2-\lambda_p}$$

Analytical** result for fluctuation within a single free protein:

$$C_x(t) = \frac{\langle \delta x(t)\delta x(0)\rangle}{\delta x(0)^2} = E_{\lambda_r}\left[-\frac{k_s}{\zeta_{r,0}(\lambda_r)\Gamma(1-\lambda_r)}t^{\lambda_r}\right]$$

$$\tau_\nu = \frac{a^2}{\nu}$$

$$\tau_B = \frac{m_p}{6\pi\mu a} \approx 0.2\tau_\nu$$

$$\tau_k = 2\pi\sqrt{\frac{m_p}{k}} \approx 0.8\tau_\nu$$

[1] Hanley et al, *J. Biol. Chem.*, 2003
[2] Min et al, *Phys. Rev. Lett.*, 2005

NC correlation functions are significantly impacted by the internal dynamics of the protein relaxation

Effects of RBC-Marginating Potential on NC Positional Distribution

$$\Phi_{RBC}(\mathbf{r}) = \int_V \rho_{RBC}(\mathbf{r}')\langle\phi\rangle_1(\mathbf{r},\mathbf{r}')d\mathbf{r}'$$

$$\langle\phi\rangle_1 = \phi_{WCA} = 4\varepsilon\left[\left(\frac{\sigma'}{r}\right)^{12} - \left(\frac{\sigma'}{r}\right)^{6} + 0.25\right]$$

$$\sigma' \le r \le r_{\min} = 2^{1/6}\sigma'$$

$$\sigma' = \frac{\sigma}{2} + a$$

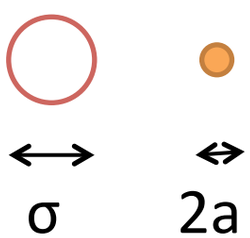

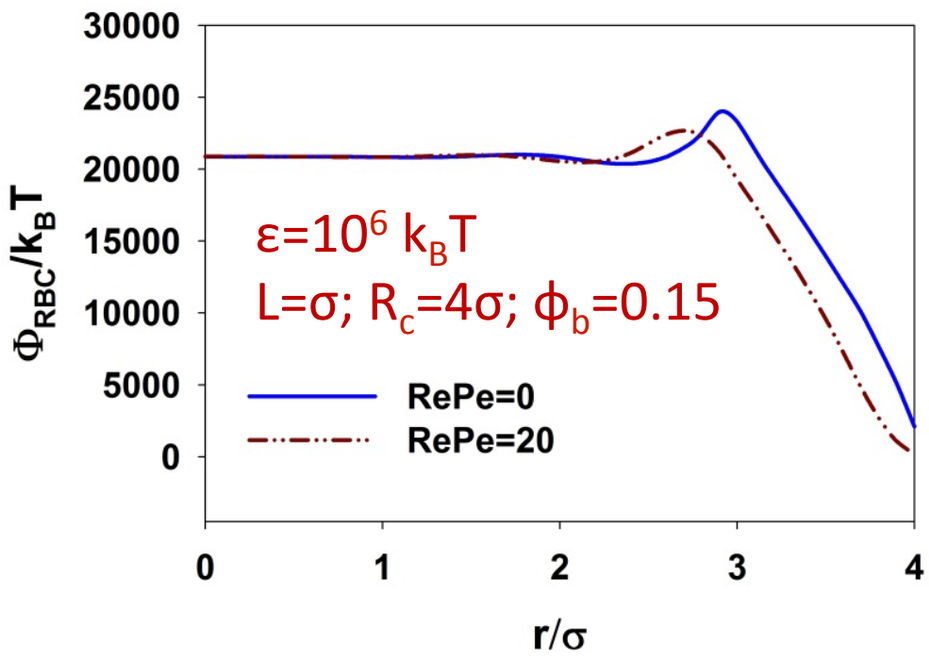

a=250 nm
k=1 N/m

$\lambda_p = \lambda_r = 0.5$
$k_s = 1.882$ N/m
$\zeta_{r,0}/k_s = 0.7\ s^{0.5}$

Position of NC

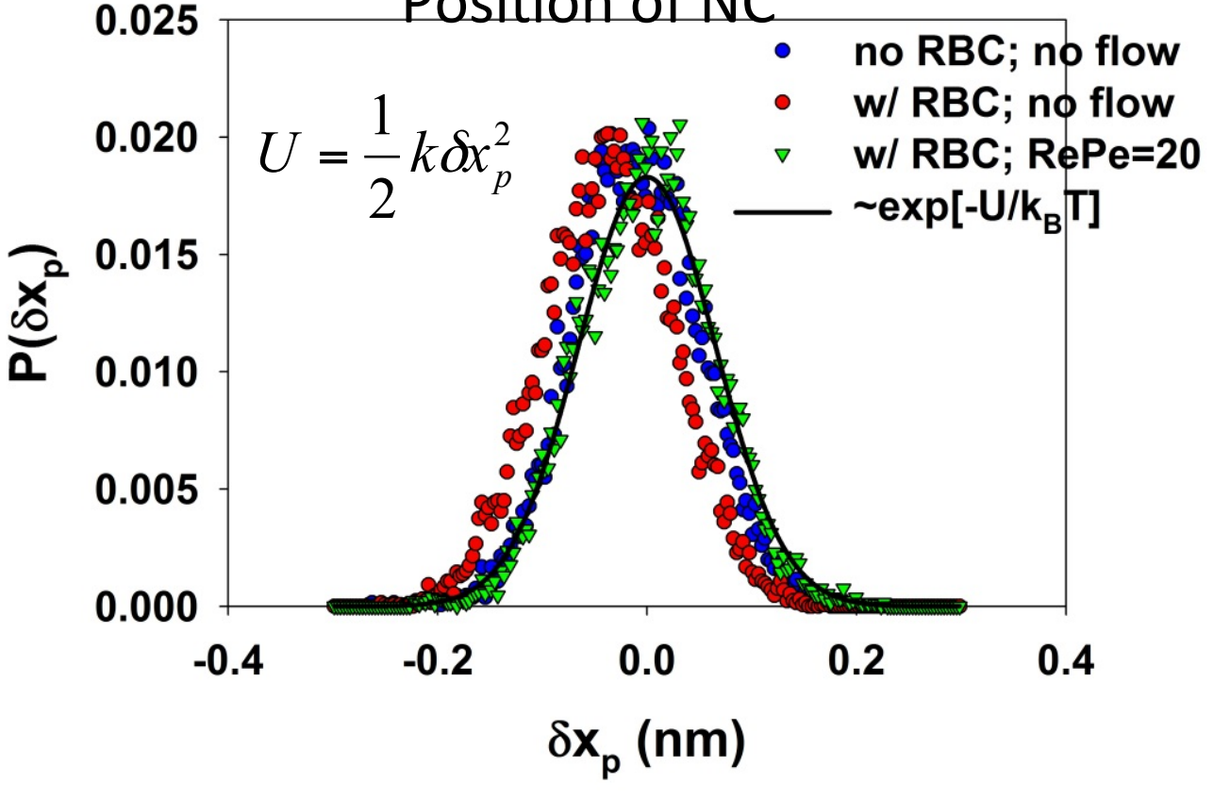

Position of receptor tip

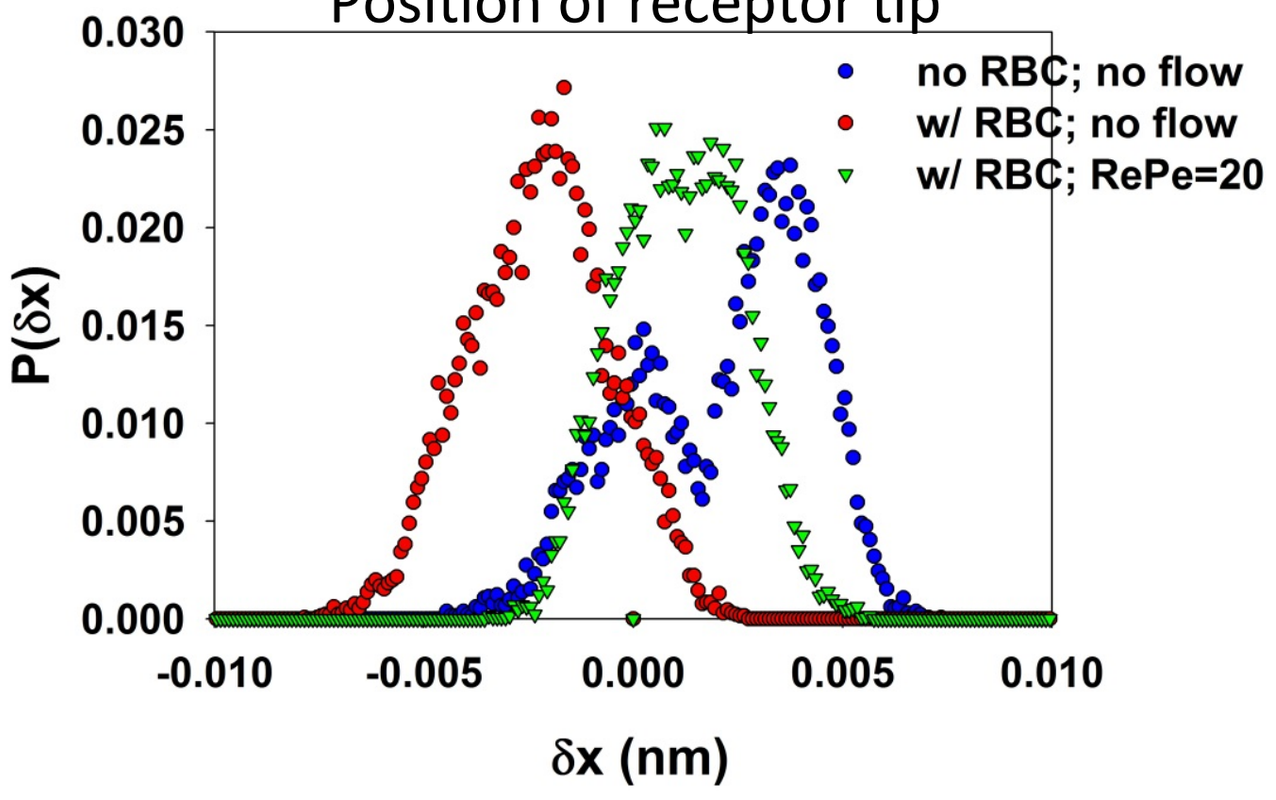

RBC-marginating potential affects binding potential energy of NC is and may influence the internal energy landscape of receptor protein

(2) Computationally Demanding but Rigorous Approach: Full Hydrodynamic Consideration using Equation-Free Brownian Dynamics (BD) and Direct Numerical Simulations (DNS)

Inner layer: DNS for full hydrodynamic equations

$$\rho^{(f)}\left[\frac{\partial \mathbf{u}}{\partial t}+\left(\mathbf{u}\cdot\nabla\right)\mathbf{u}\right]=-\nabla p+\nabla\cdot\boldsymbol{\tau} \qquad \nabla\cdot\mathbf{u}=0$$

The mobility tensor is computed ab initio using DNS and the dynamics of particles are evolved using BD

Outer wrapper for type-1 particles:
coarse integration of equations of motion for blood cells

$$\Delta\mathbf{x}_i^{(1)}=\left\{\mathbf{U}_i^{(1)}+\sum_{j=1}^{N_1}\left[\frac{\mathbf{D}_{ij}^{(11)}}{k_BT}\cdot\mathbf{F}_j^{T1}+\nabla_j\cdot\mathbf{D}_{ji}^{(11)}\right]\right\}\Delta T_1 \quad\Rightarrow\quad \rho_{RBC}\left(\mathbf{r},t\right)$$

Outer wrapper for type-2 particles:
coarse integration of equations of motion for NC

$$\left\langle\Delta\mathbf{x}_i^{(2)}\right\rangle_{N_1}=\left\{\left\langle\mathbf{U}_i^{(2)}\right\rangle_{N_1}+\sum_{j=1}^{N_2}\left[\left\langle\frac{\mathbf{D}_{ij}^{(22)}}{k_BT}\cdot\mathbf{F}_j^{T2}\right\rangle_{N_1}+\left\langle\nabla_j\cdot\mathbf{D}_{ji}^{(22)}\right\rangle_{N_1}\right]+\nabla_i\boldsymbol{\Phi}_{RBC}\left(y_i,\mathbf{r}^{N_2}\middle|\mathbf{r}^{N_1}\right)\right\}\Delta t+\left\langle\mathbf{x}_{Bi}^{(2)}(t)\right\rangle_{N_1}$$

$$\left\langle\mathbf{x}_{Bi}^{(2)}(t)\mathbf{x}_{Bj}^{(2)}(t)\right\rangle=2\mathbf{D}_{ij}^{(22)}k_BT\Delta t \qquad \left\langle\mathbf{x}_{Bi}^{(2)}(t)\right\rangle_{N_1}=0 \quad\Rightarrow\quad \rho_{NC}\left(\mathbf{r},t\right)$$

Kevrekidis et al, *AIChE J.*, 2004

Brady and Bossis, *Ann. Rev. Fluid Mech.*, 1988; Banchio and Brady, *J. Chem. Phys.*, 2003

Multivalent Complexes and Nanogels

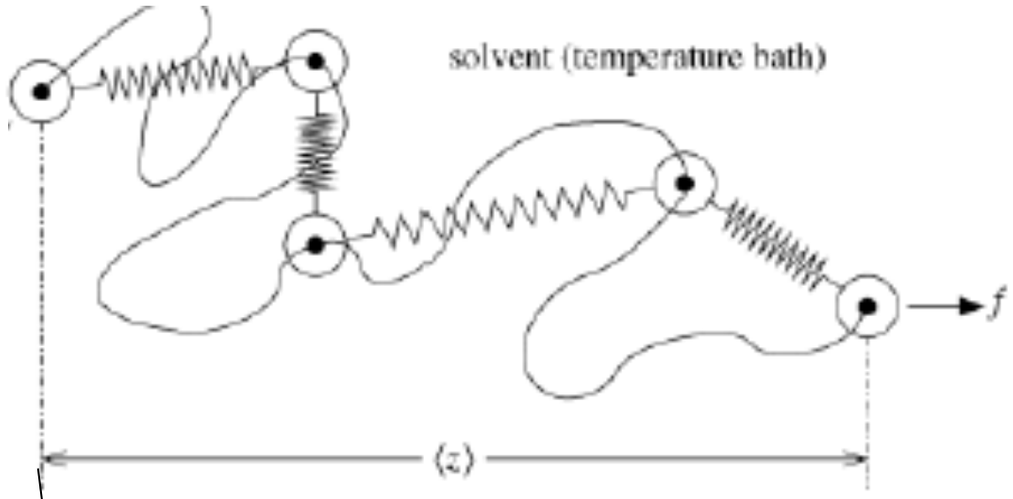

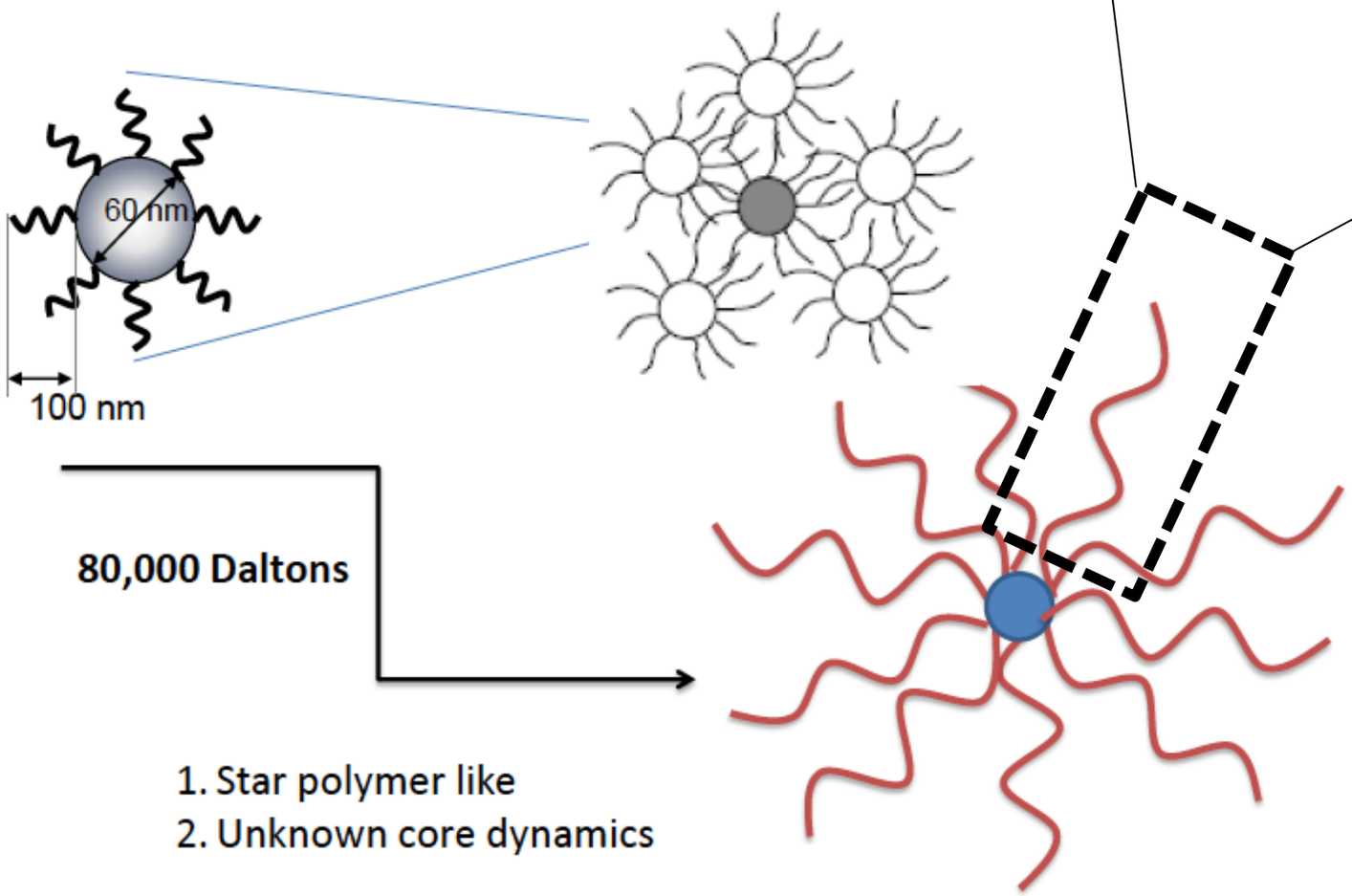

Brownian Dynamics Model

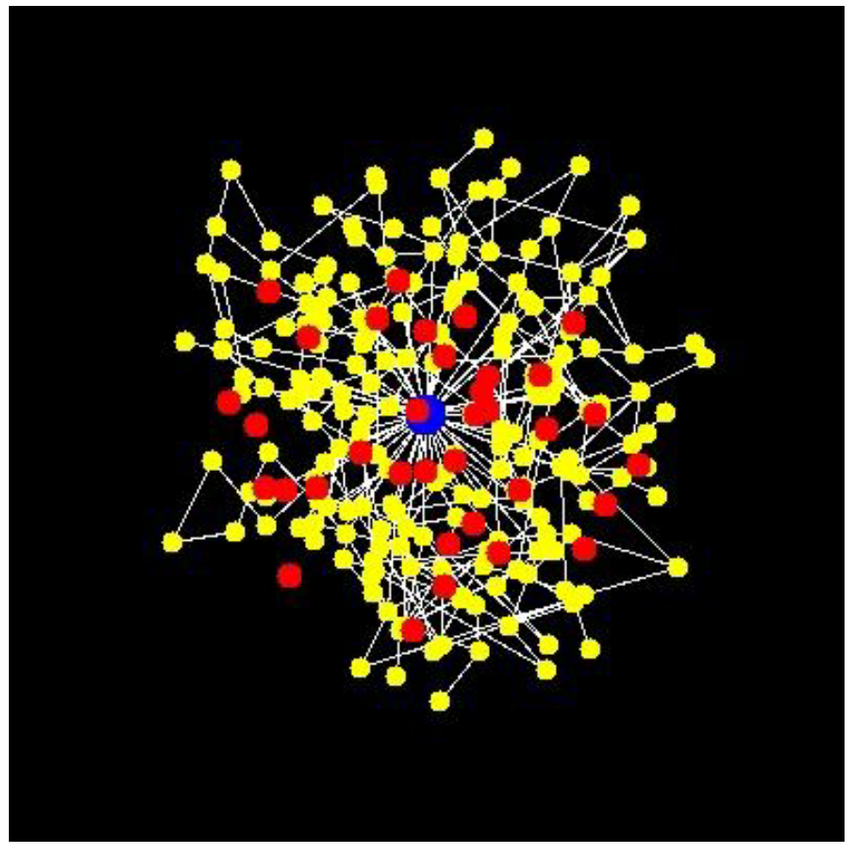

Nanogel Internal Hydrodynamics

- Conformation
- Deformation with flow, adhesion
- Diffusivity, Structure relaxation

Nano-gel under shear [1]

Deformation at Pe=5

Entanglement density = 20%

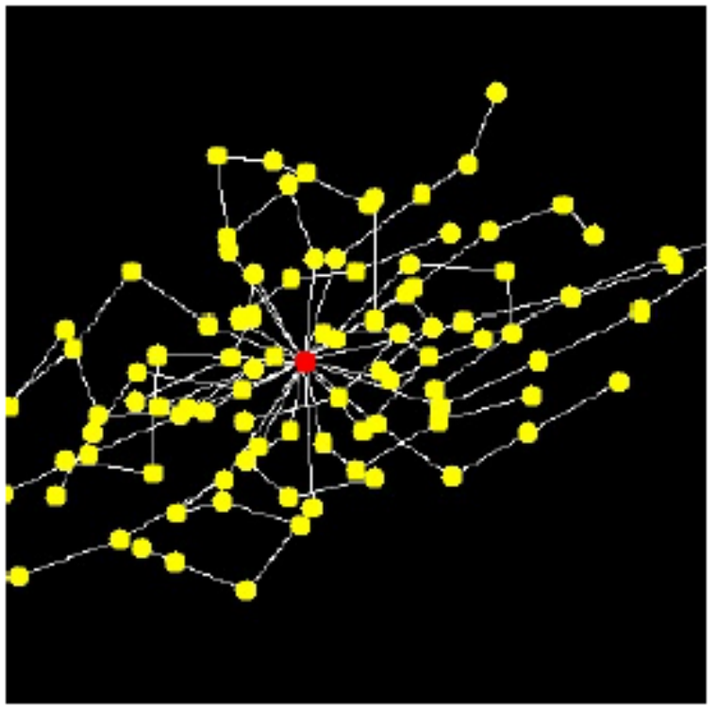

Entanglement density = 60%

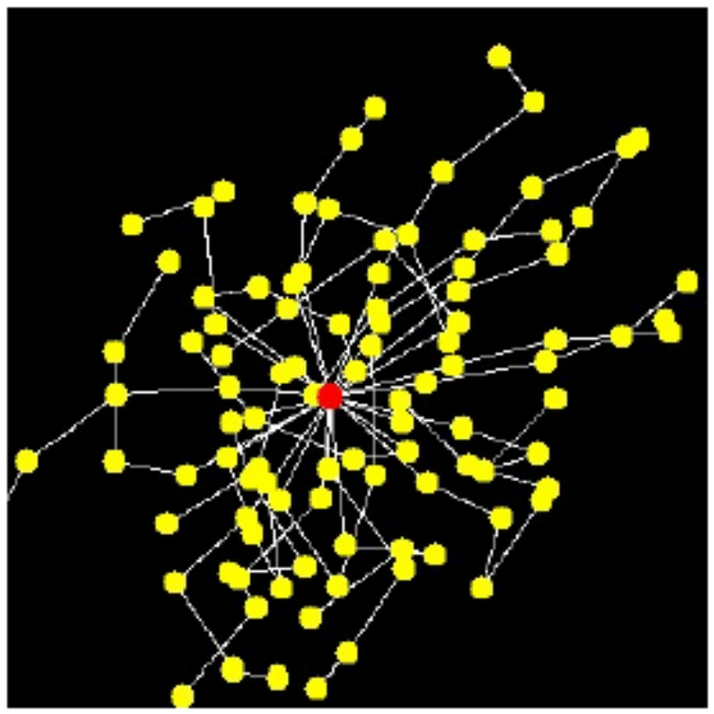

Entanglement density = 100%

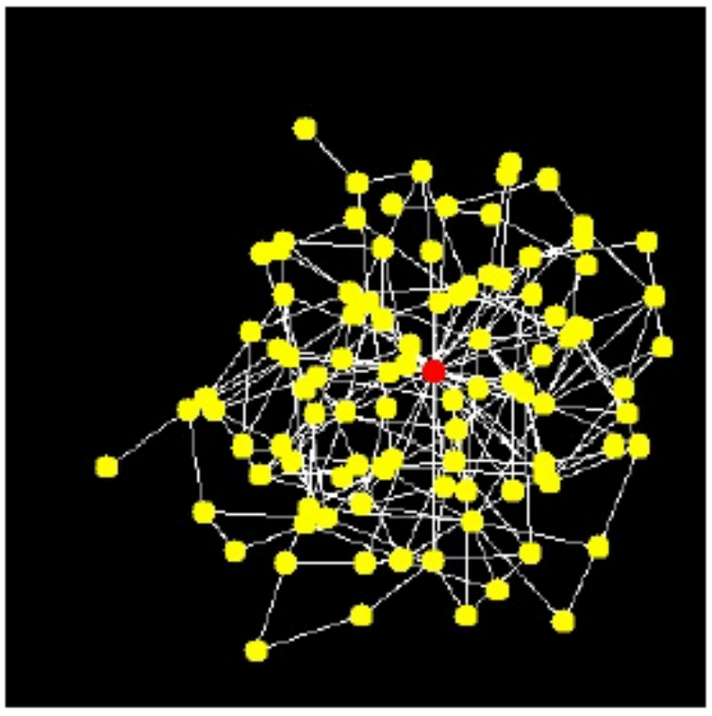

Entanglement density = 160%

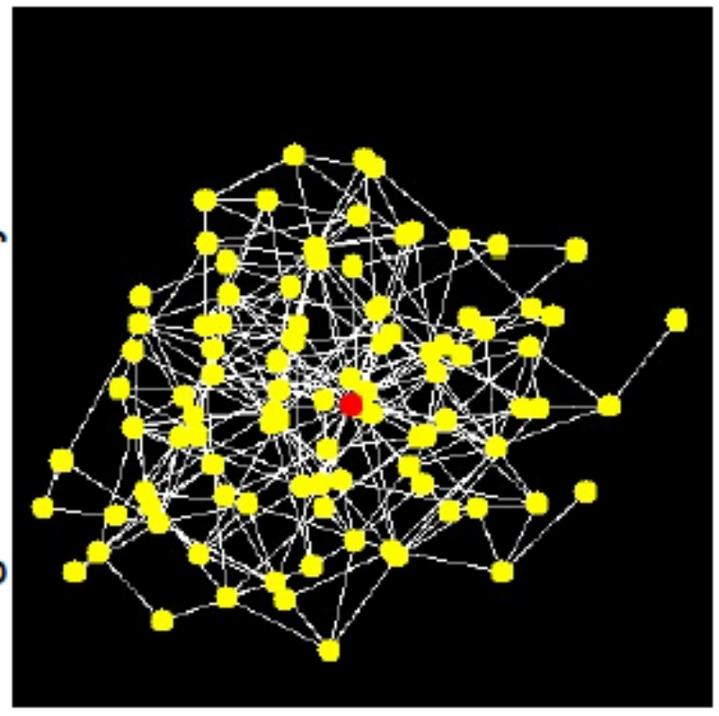

[1] *Pe* is based on *a* i.e. $Pe = \frac{ua}{D_0}$.

Penn

Nanoscale Fluctuating Hydrodynamics: Direct Numerical Simulation (DNS) to Treat Hydrodynamic Interactions and Stochastic Fluctuations

Governing equations for the fluid motion and rigid particles

$$\nabla\cdot\mathbf{u}=0$$

$$\rho_f\frac{D\mathbf{u}}{Dt}=\rho_f\mathbf{f}+\nabla\cdot\sigma=0$$

$$\sigma=-p\mathbf{I}+\mu\left[\nabla\mathbf{u}+\left(\nabla\mathbf{u}\right)^T\right]+\underline{S}$$

(Random Stress)

(Landau and Lifshitz, *Fluid Mechanics*, 1959)

$$m_i\frac{d\mathbf{U}_i}{dt}=-\int_{\partial\Omega_i(t)}\sigma\cdot\mathbf{n}\,ds$$

$$\frac{d\left(\mathbf{I}_i\omega_i\right)}{dt}=-\int_{\partial\Omega_i(t)}\left(\mathbf{x}-\mathbf{X}_i\right)\times\left(\sigma\cdot\mathbf{n}\right)ds$$

Boundary conditions

$$\mathbf{u}=0\ \text{on}\ \left(\partial\Omega\right)_u$$

$$\sigma\cdot\mathbf{n}=0\ \text{on}\ \left(\partial\Omega\right)_\sigma$$

$$\mathbf{u}=\mathbf{V}_i+\omega_i\times\left(\mathbf{x}_i-\mathbf{X}_i\right)\ \text{for}\ \mathbf{x}\in\partial\Omega_i(t)$$

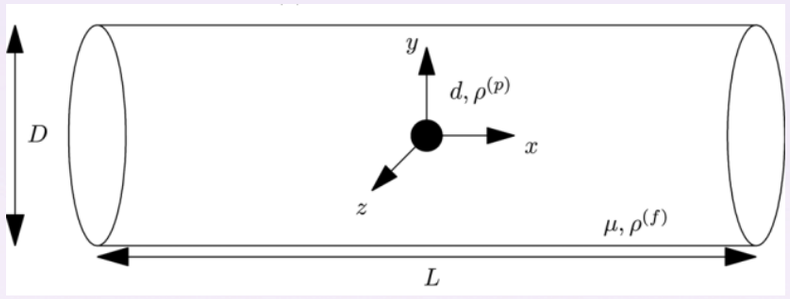

Initial conditions

$$\mathbf{u}=\mathbf{u}_0\ \text{on}\ \Omega_0(0)$$

$$\left\langle S_{ij}\right\rangle=0;\ \left\langle S_{ik}\left(\mathbf{x}_1,t_1\right)S_{lm}\left(\mathbf{x}_2,t_2\right)\right\rangle=2k_BT\mu\left(\delta_{il}\delta_{km}+\delta_{im}\delta_{kl}\right)\delta\left(\mathbf{x}_1-\mathbf{x}_2\right)\delta\left(t_1-t_2\right)$$

Hydrodynamic Interactions and Adhesive Interactions can be Simultaneously Modelled using Fluctuating Hydrodynamics

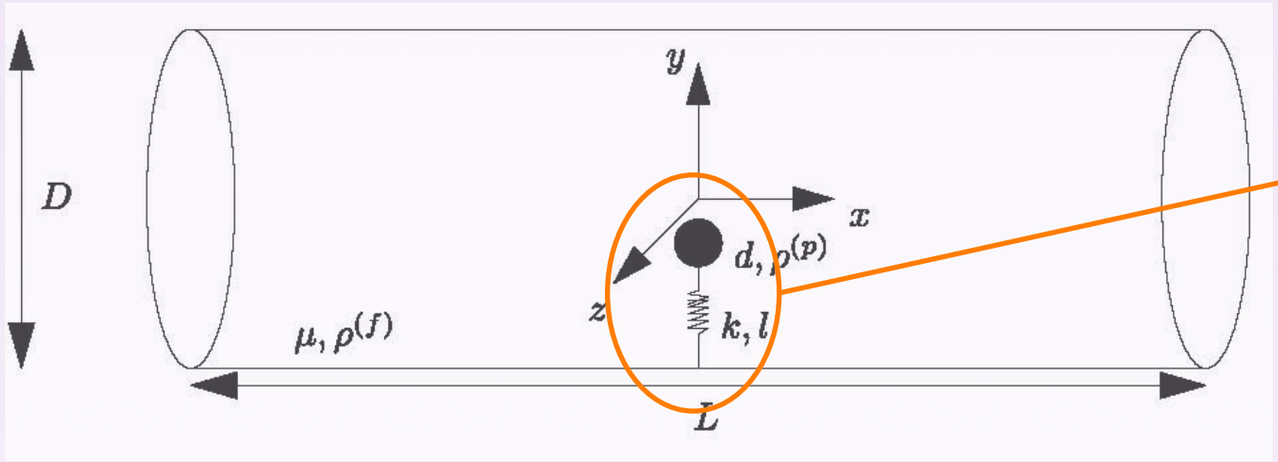

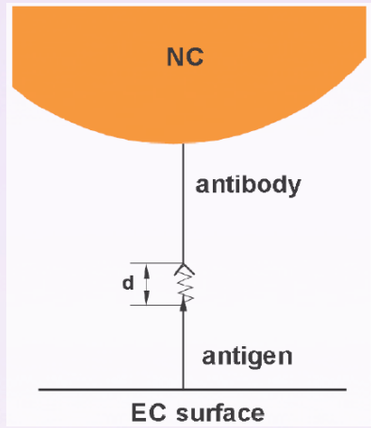

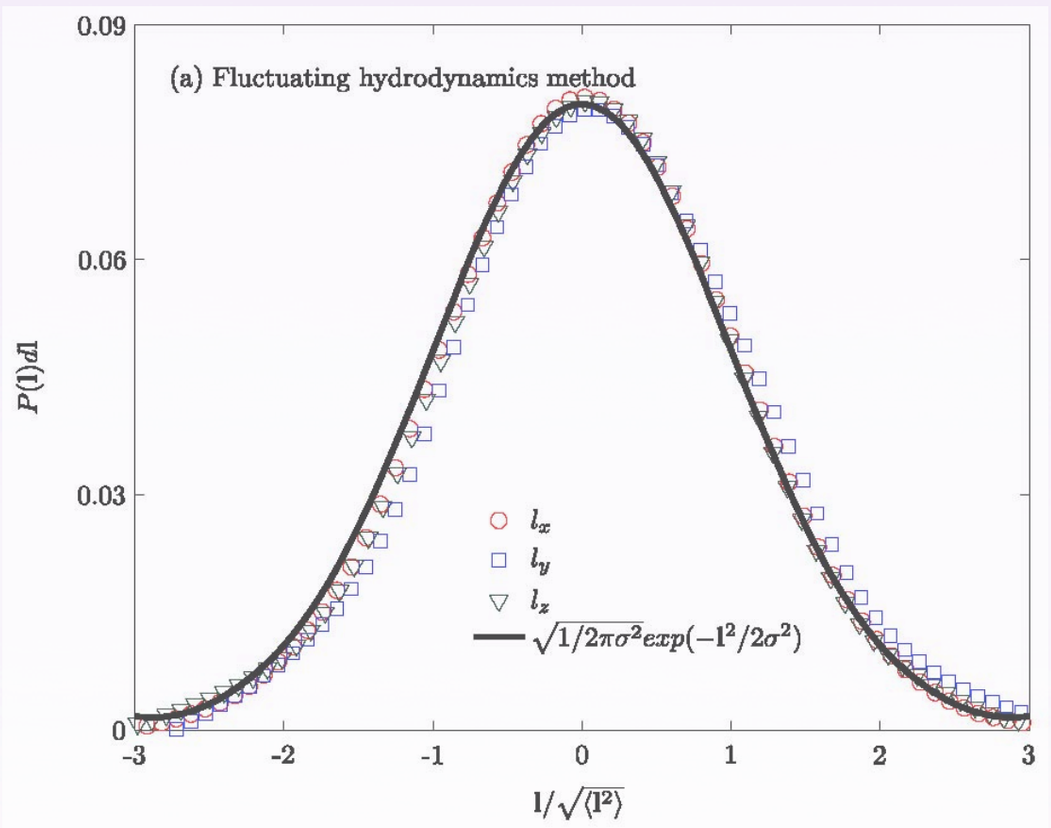

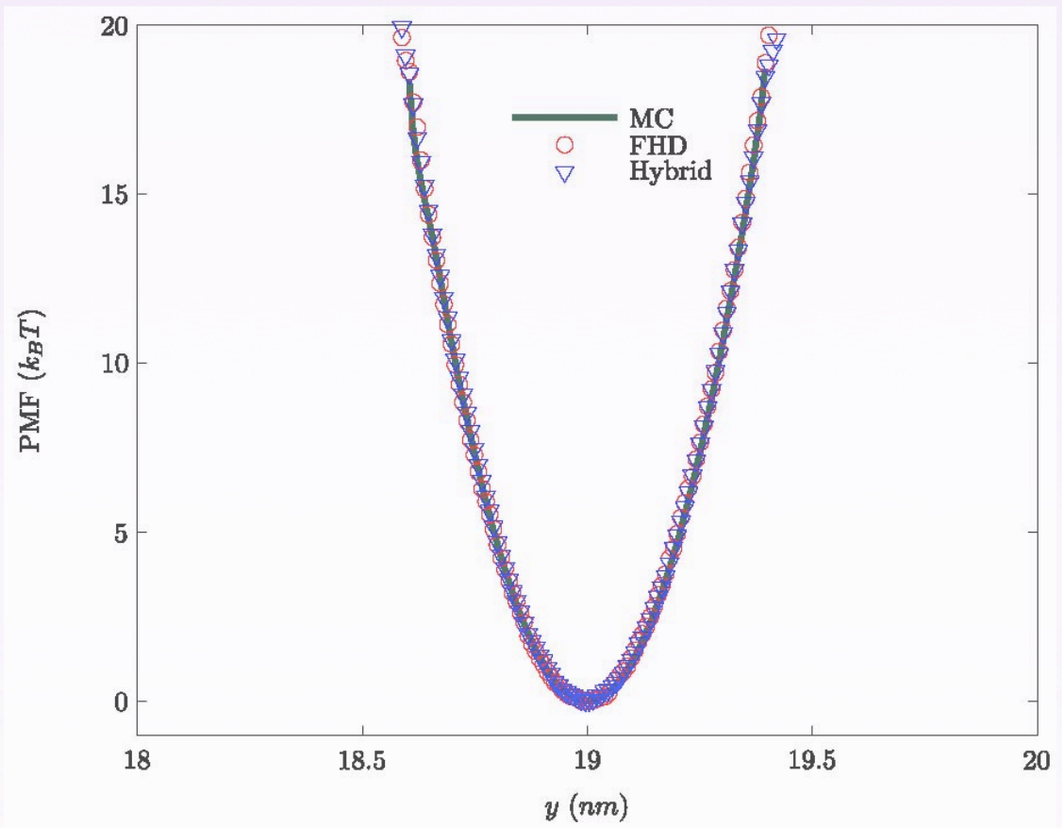

The Potential Mean Force (PMF) between NC and adhesive cell surfaces based on Metropolis Monte Carlo and the weighted histogram analysis method is compared with free energy obtained using fluctuating hydrodynamics and hybrid methods. The agreement is excellent.

Radhakrishnan, Uma, Liu, Ayyaswamy, Eckmann, J. Comp. Phys, 2013

Multibody Hydrodynamic Interactions

Data for arterioles and venues

Theoretical data		Calculation input
Vessel diameter: D (μm)	20–50	20
Average velocity: U_{av}	0.2–5 cm/s	$U_{max}=10^4$μm/s
RBC hematocrit: H_{ct}	0.2–0.3	
Relative viscosity: $\mu_{rel}=\mu/\mu_{plasma}$	1.5–1.8	5.6 10^6μm^2/s

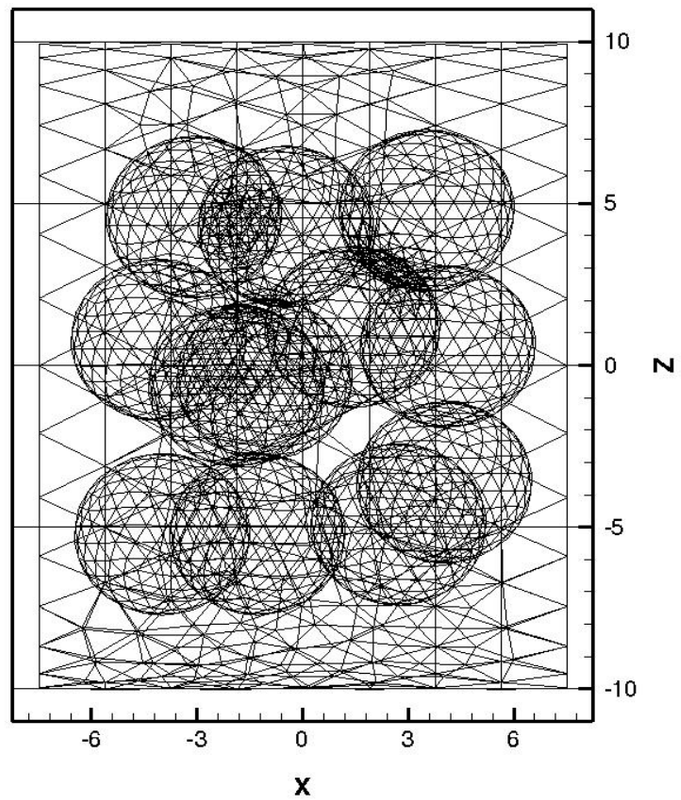

Data for hard sphere suspension

Volume fraction: ϕ_b	0.15–0.2	0.17 (0.1, 0.15, 0.2)
Cell diameter: σ (μm)	4.3–5.2	5
D_pipe/d_part	3.8–11.6	4

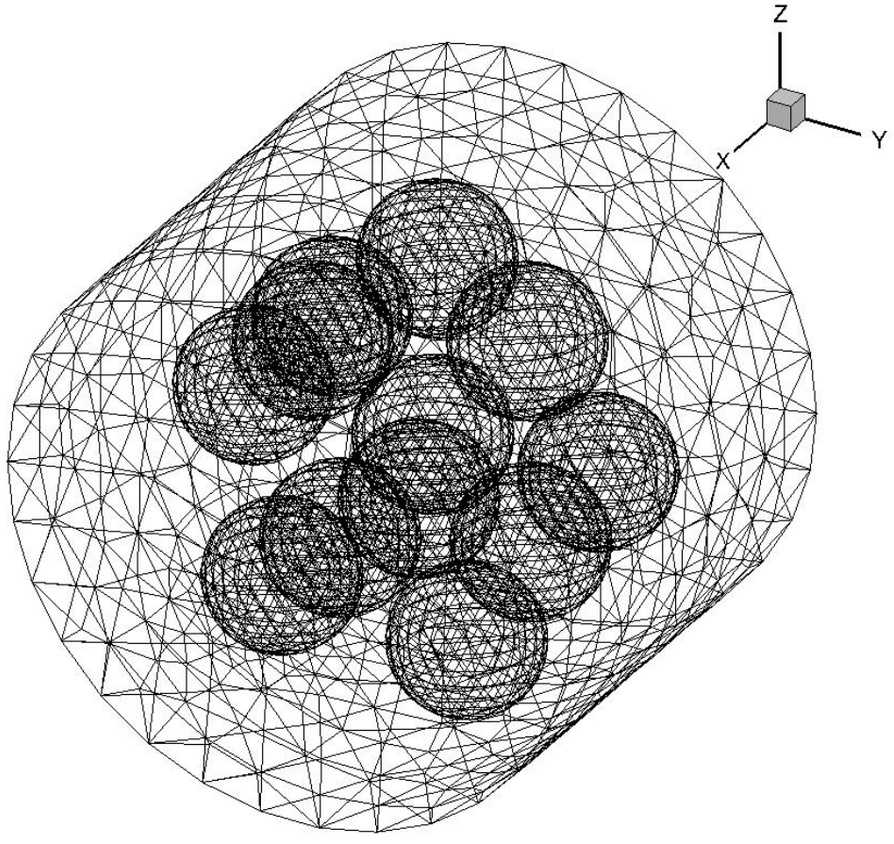

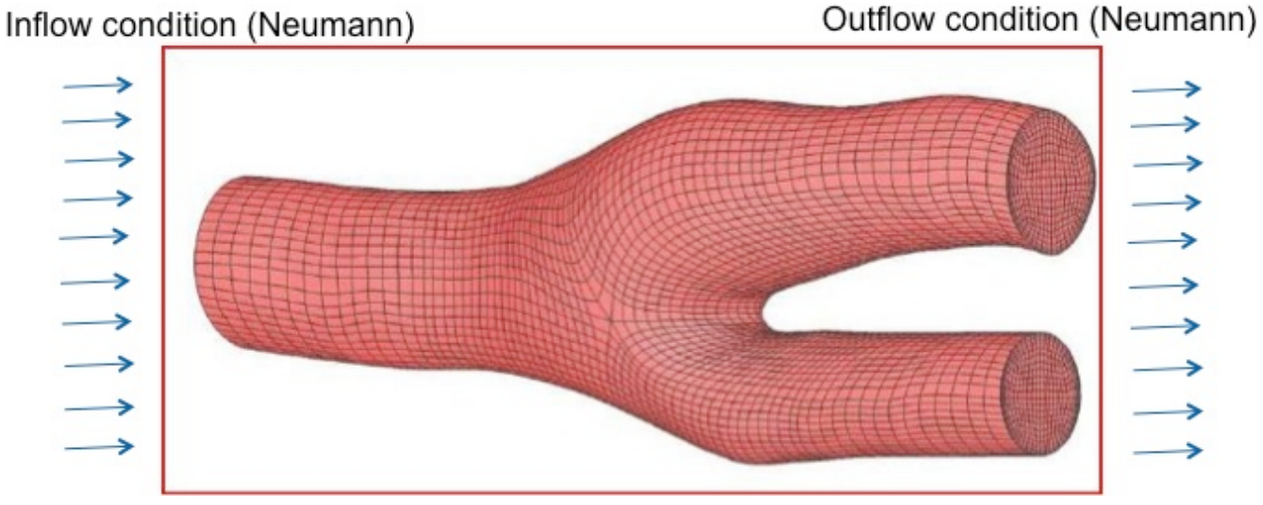

Towards a Pharmacological Model

- 3D generalized Langevin dynamics with membrane thermal fluctuations for NC rolling and internalization
- Combining with molecular dynamics of receptor protein for probing dynamic viscosity of confined water
- DDFT closure for anisotropic particles
- Better treatment of HI through the use of direct numerical simulations + Brownian Dynamics
- Realistic Adhesion Model for NC Avidity

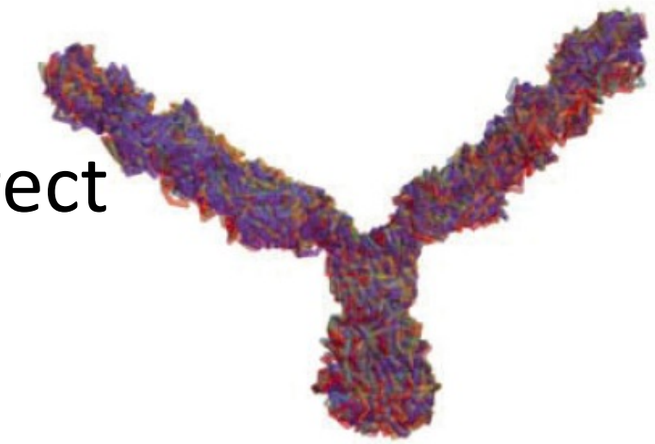

ICAM-1

Support: NSF, NIH/NIBIB, XSEDE

Extreme Science and Engineering Discovery Environment

THANK YOU!